

The Rainy Continental Snow climate: Global comparison with 40 years of snow cover modeled in the Chic-Chocs, northeastern Appalachians mountains.

Francis MELOCHE^{1,2,3}, Benjamin IMBACH^{1,2,3}, Jean-Benoît MADORE^{2,3}, Benjamin REUTER^{4,5}, Alexandre LANGLOIS^{2,3} and Francis GAUTHIER^{1,2}

¹*Laboratoire de Géomorphologie et de gestion des risques en montagnes (LGGRM), Département de Biologie, Chimie et Géographie, Université du Québec à Rimouski, Canada.*

²*Center for Nordic studies, Université Laval, Canada.*

³*Groupe de Recherche Interdisciplinaire en Milieux Polaire (GRIMP), Département de Géomatique, Université de Sherbrooke, Canada.*

⁴*Univ. Grenoble Alpes, Univ. de Toulouse, Météo-France, CNRS, CNRM, Centre d'Études de la Neige, Grenoble, France.*

⁵*Météo-France, Direction des opérations pour la prévision, Toulouse, France.*

Correspondence: Francis Meloche <francis_meloche@uqar.ca>

ABSTRACT. This study provides a comprehensive analysis of the snow and avalanche climate of the Chic-Chocs region of the Gaspé Peninsula, located in the northeastern Appalachians of eastern Canada. The data revealed two major components of the snow climate: a cold snow cover combined with a maritime influence causing melt/ice layers through rain-on-snow events. The CRCM6-SNOWPACK model chain was good at representing the seasonal mean of climatic indicators, snow grain size and a snow problem type that well represented the snow climate of the study region. The global comparison shows that the snow climate is different from other areas in western North America, but similar to Mt. Washington (New Hampshire, USA) and central Japan. We show a clustering based solely on avalanche problem types, which showed that the onset date of wet snow problems divided most of the winter into three clusters. We compare these clusters with the French Alps and show

28 **some similarities, moving away from a traditional snow climate description.**
29 **The paper concludes that the use of advanced snow cover modeling combined**
30 **with the Reuter and others (2022) method represents a new potential frame-**
31 **work to improve our understanding and classification of snow climates, ulti-**
32 **mately contributing to improved forecasting and risk management in similar**
33 **regions.**

34 INTRODUCTION

35 Snow climate classifications were initially developed to characterize the climate of mountainous regions,
36 often to understand the conditions driving avalanche hazard (Armstrong and Armstrong, 1987; LaChapelle,
37 1965; McClung and Schaerer, 2006; Roch, 1949). In hydrology and climate modeling, the term "snow
38 climate" has been employed to delineate seasonal average snow cover properties, including total depth,
39 presence of depth hoar, ice layers, and snow temperature (Sturm and others, 1995). Within the field
40 of snow avalanche studies, the term "snow climate" specifically denotes the properties of the snow cover
41 that are relevant for the formation of snow avalanches (Hägeli and McClung, 2003). Understanding the
42 snow climate classification of a given mountain region is essential for developing location-specific avalanche
43 mitigation and forecasting programs (e.g. McClung and Schaerer, 2006).

44 The snow climate classification has three primary patterns: Maritime, Continental, and Transitional
45 (LaChapelle, 1965). The Maritime snow climate is characterised by warm temperatures and heavy snowfall,
46 with major instabilities predominantly attributed to recent snow loading in the upper snow cover (Haegeli
47 and McClung, 2007; Mock and Birkeland, 2000). Avalanche forecasting programs in these regions heavily
48 rely on weather observations (McClung and Schaerer, 2006). Conversely, the Continental snow climate is
49 distinguished by cold temperatures and light snowfall, featuring weak persistent layers in the snow cover
50 that necessitate systematic monitoring for forecasting snow avalanches (McClung and Schaerer, 2006).
51 The Transitional snow climate exhibits characteristics of both Maritime and Continental snow climates
52 (Haegeli and McClung, 2007). However, the description of a transitional snow climate is often generalized
53 and has been primarily delineated in western North America, Haegeli and McClung (2007) suggest that
54 other regions experiencing varying degrees of continental and maritime influences should be included to
55 enrich the understanding of this transitional snow climate.

56 Mock and Birkeland (2000) introduced a flowchart aimed at classifying snow climates, outlining snow
57 cover processes pertinent to avalanche hazard assessment. Their approach utilized meteorological data to
58 categorize individual winter seasons into distinct snow climates. However using only meteorological data
59 is insufficient to describe snow instability, as Schweizer and others (2003) demonstrated that the physical
60 properties of slabs and weak layers serve as critical indicators of avalanche formation (Hägeli and McClung,
61 2003). Recognizing this, Haegeli and McClung (2007) emphasized the necessity of incorporating additional
62 snow stratigraphy information to refine the description of snow climates. They proposed expanding the
63 Mock and Birkeland (2000) flowchart to integrate avalanche and snow observations, particularly focusing
64 on persistent weak layer observations, thus introducing the term "snow and avalanche climate" (Haegeli
65 and McClung, 2007). This inclusion provides valuable insights into the percentage of avalanche activity
66 on persistent weak layers and the specific types of persistent weak layers characterizing each snow and
67 avalanche climate zone. This refinement is especially pertinent in delineating Transitional snow climates,
68 where the interplay of Continental and Maritime influences leads to distinctive persistent weaknesses in
69 particular regions.

70 The concept of "avalanche problem types" refers specific weather events and snow cover properties char-
71 acterizing different types of avalanche problems, such as wind slab or persistent slab avalanche problems
72 Statham and others (2018); EAWS (2019). These avalanche problem types represent the primary concern
73 for avalanche forecasters regarding specific meteorological and snow cover conditions. They are the founda-
74 tion for various avalanche operational hazard forecasting to communicate the avalanche hazards in North
75 America (Statham and others, 2018), and Europe (Techel and others, 2020).

76 Building upon this framework, Shandro and Haegeli (2018) integrated avalanche problem data type
77 with the Mock and Birkeland (2000) flowchart to enhance the characterization of snow avalanche hazard in
78 western Canada. While the methodology of Mock and Birkeland (2000) offers a generalized description of
79 snow climate across multiple winter seasons, the incorporation of avalanche problem type data facilitates
80 a more nuanced understanding, addressing daily concerns for forecasters throughout the season. However,
81 building a temporally extensive database of forecast avalanche problem types can be difficult without
82 avalanche forecasting data. To fill this gap and to provide an independent methodology, Reuter and
83 others (2022) proposed a method to derive avalanche problem types from snow cover model output such as
84 SNOWPACK (Lehning and others, 1999) or SURFEX/CROCUS (Vionnet and others, 2012). This method
85 allows to characterise based on weather forecasting reanalysis data and snow cover modeling, for instance,

86 and hence, omitting the use of forecasting data.

87 Various combinations of the methodologies outlined above have been employed to describe and classify
88 additional regions, utilizing different data types primarily based on data availability. For instance, Ikeda
89 and others (2009) utilized the Mock and Birkeland (2000) flowchart alongside snow cover data to delineate
90 the snow climate of the Japanese Alps. Their findings for the Japanese Coastal mountains exhibited
91 similarities with the Maritime climate zone. However, the Central Japanese Alps, characterised by a thin
92 snow cover, cold temperatures conducive to persistent weakness development, and a significant amount of
93 rainfall, did not align with any of the three main snow climates. Consequently, they introduced the term
94 "Rainy Continental" for the Central Japanese Alps (Ikeda and others, 2009). Similarly, Eckerstorfer and
95 Christiansen (2011) utilized snow profile data to describe the snow climate of Svalbard's main settlement,
96 Longyearbyen. Their analysis highlighted a thin snow cover, persistent weaknesses, and substantial ice
97 layers attributed to maritime influences, which led them to propose the term "High Arctic Maritime" for
98 Central Svalbard (Eckerstorfer and Christiansen, 2011). Recently, Reuter and others (2023) characterized
99 the snow climate of the French alps using two approaches, the snow climate classification algorithm of
100 Mock and Birkeland (2000) and using avalanche problem types based on snow cover simulations. With
101 their approach, they put forward the idea of classifying snow and avalanche climates based on avalanche
102 problem type occurrences. Their comparisons with the standard snow climate classification suggests that
103 in the French alps avalanche problem occurrences provide for a more detailed characterisation.

104 In eastern Canada, The Chic-chocs mountains in the Gaspé Peninsula are prone to snow avalanches.
105 Multiple studies have highlighted the influence of snowstorms and thaw events on the local snow avalanche
106 dynamic (Fortin and others, 2011; Gauthier and others, 2017; Germain and others, 2009; Hétu, 2010).
107 Despite the Köppen classification indicating a humid continental climate, the region experiences a signif-
108 icant maritime influence, complicating the classification of the snow and avalanche climate (Fortin and
109 others, 2011; Gagnon, 1970; Gauthier and others, 2017). While the winter climate of the region has been
110 extensively documented (Fortin and others, 2011; Fortin and Hétu, 2014; Gagnon, 1970; Gauthier and
111 others, 2017), the description primarily relies on seasonal average climate conditions not directly relevant
112 to avalanche formation. Hence, comprehensive analysis integrating snow cover and weather data relevant
113 to avalanche formation holds promise to elucidate the region's snow and avalanche climate.

114 Given the presence of established approaches in snow climatology and the importance to better under-
115 stand the snow and avalanche climate of the Chic-Chocs mountains, we aim at the following objectives:

116 1) Describe the snow and avalanche climate for the Chic-Chocs mountains, 2) Compare the dataset Chic-
117 Chocs region with other mountain ranges such as Mount Washington (New Hampshire, USA), Central
118 Japan and the French Alps. We conclude the paper by discussing how the current snow climate observed
119 in the Chic-Chocs could evolve regarding climate change.

120 **Study area**

121 This study focuses on the Chic-Chocs mountains, a northern extension of the Appalachian Mountains,
122 which forms an inland massif serving as the backbone of the Gaspé peninsula (Figure 1). This central
123 massif comprises sub-alpine and alpine terrain, ranging in elevation from 800 to 1200 meters above sea
124 level (m a.s.l.), and is encompassed by a lower plateau situated at 400-500 m a.s.l. (Figure 1). The
125 study area is mainly the Avalanche Québec forecasting area. This non-profit organization has been issuing
126 avalanche bulletins for backcountry users in the Chic-Chocs since 2000. Since Avalanche Québec is now
127 part of the Avalanche Canada forecasting program, the organisation will benefit from a snow and avalanche
128 climate to inform hazard forecasting as well as risk management in the region, while such procedures were
129 established in the climate regions of Western Canada.

130 The Chic-Chocs region receives approximately 800 mm of precipitation annually, while the high plateau
131 of the interior receives around 1,600 mm (Fortin and others, 2011; Gagnon, 1970; Germain and others,
132 2010). Snowfall typically occurs from December to April, accompanied by an average of about 60 mm of
133 rainfall per winter (Fortin and others, 2011). The mean annual temperature, spanning from 1971 to 2010,
134 varies from 3°C along the Gaspé North Coast to -4°C at 1268 m (Mt Jacques-Cartier) (Gray and others,
135 2017). The regional climate exhibits contrasting weather patterns: 1) cold Arctic air masses often bring
136 northwesterly winds with temperatures dropping below -20 °C, and 2) continental low-pressure systems,
137 usually accompanied by northeasterly winds, resulting in temperatures near the freezing point and potential
138 rain. These weather systems, commonly referred to as the Alberta Clipper, the Colorado Low, and the
139 Hatteras Low, significantly influence the Gaspé Peninsula's weather, impacting the type of precipitation
140 experienced in the area (Fortin and Hétu, 2014). The interaction of these weather patterns with the
141 peninsula's topographic features creates a snow accumulation pattern conducive to avalanche formation
142 (Germain and others, 2010). Most avalanches in the region are natural releases occurring during storms
143 (Fortin and others, 2011; Gauthier and others, 2017; Germain and others, 2009; Hétu, 2010).

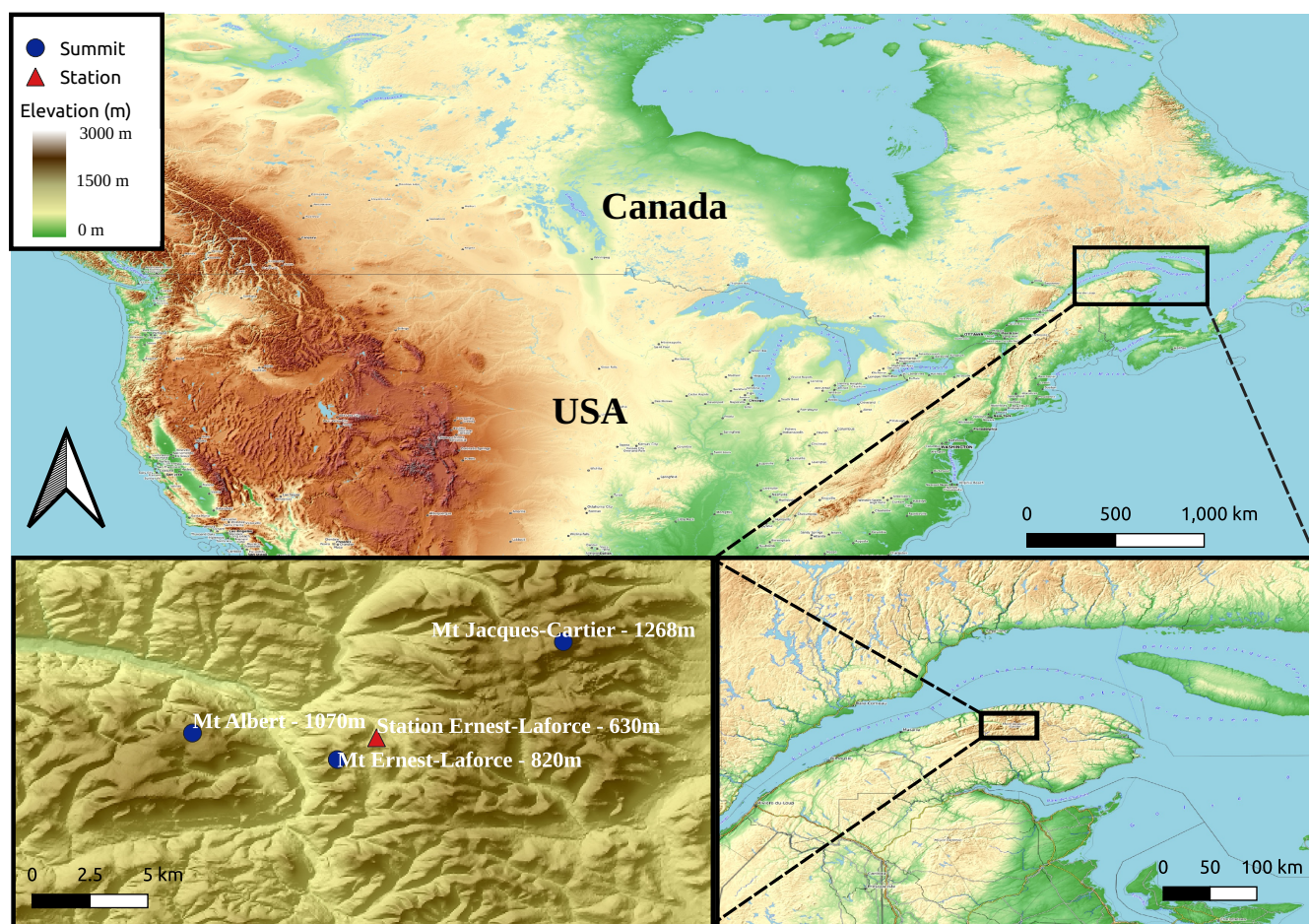


Fig. 1. Localisation map of the study inside North America. The input represents different spatial scale of the study area with the different summits around the weather station Ernest-Laforce 630 m.

144 METHODS

145 **Classification strategy**

146 To provide a comprehensive description of the snow and avalanche climate, we used several methodologies
147 drawn from work on snow and avalanche climatology widely used over the past decades (Mock and Birke-
148 land, 2000; Shandro and Haegeli, 2018; Sturm and others, 1995; Reuter and others, 2022). While these
149 methodologies formed the basis of our approach, we adapted them by selectively incorporating relevant
150 aspects tailored to our specific research needs. This approach integrated several types of data relevant to
151 understanding avalanche formation.

152 We used the Mock and Birkeland (2000) flowchart, which uses meteorological data to outline the general
153 snow climate. We then retrieved from snow cover simulations the distribution of snow grain types for the
154 whole snow cover described by Sturm and others (1995), but also for the critical weak layers. These snow
155 cover data not only clarify the dominant metamorphic processes, but also help to identify which snow grain
156 types characterised the weak layers of the study area. In addition, we have included avalanche problem
157 types to characterize avalanche hazard, inspired by the approach of Shandro and Haegeli (2018). The
158 avalanche problem types were derived from simulations with the SNOWPACK model (Lehning and others,
159 1999), following the framework described in Reuter and others (2022). They characterize snow instability
160 patterns for every day. This type of data serves complements the description of the snow climate.

161 Finally, similarly to Reuter and others (2023), a temporal cluster analysis has been performed over
162 the 40-year period, based on the avalanche problem type. This analysis should show the different types
163 of winters that the region can experience, while providing a different point of view from the classic snow
164 climate classification of Mock and Birkeland (2000). It is important to note that the database includes
165 data representing the winter avalanche regime from December 1 through March 31. Data representing the
166 spring avalanche regime were not included in this analysis.

167 **Meteorological data**

168 Meteorological data were collected at a weather station located in the Chic-Chocs range. The weather
169 station, named Ernest-Laforce weather station (CAELA), is located on the north slope of Mt Ernest-
170 Laforce at 630 m a.s.l. (Figure 4). The data set covers the winter seasons from December 1 to March 31 for
171 the winter seasons 2012-13 to 2021-22. Hourly data for mean air temperature, snow depth, and precipitation

172 (measured by a weighing precipitation gauge) were used to calculate the meteorological variables required
173 for the Mock and Birkeland (2000) flow chart: daily mean air temperature ($^{\circ}\text{C}$), total snowfall (cm), total
174 precipitation (mm), total snow water equivalent (SWE in mm), and mean December temperature gradient
175 ($^{\circ}\text{C}/\text{m}$). Rainfall and SWE were derived from total precipitation using a rain/snow threshold of 1.2°C
176 with the hourly mean air temperature. To minimize the misclassification of precipitation events - which
177 could lead to erroneous snow- climate classification - snow events were confirmed by a significant increase
178 (> 2 cm) in snow height within the next two hours following the precipitation event. Rain events were
179 similarly validated by stable or decreasing snow height (0 cm or 1 cm). Snow depth was measured hourly
180 using an ultrasonic snow depth sensor (SR50 from Campbell Scientific) on an automated weather station.
181 Snowfall was processed as the difference between each hour and then summed for the entire season. The
182 mean temperature gradient in December was determined using the mean air temperature and snow depth
183 for December, assuming zero degree Celsius at the snow-soil interface Mock and Birkeland (2000). The
184 observed meteorological indicators used in the Mock and Birkeland (2000) algorithm are used as a basis
185 for comparing the same meteorological indicators derived from the climate simulation presented below.

186 **Climate simulation data**

187 We choose to use climate simulation data to extend the temporal scope of our study from 1982 to 2022.
188 These climate models represent different components of the climate system, such as the atmosphere, ocean,
189 land surface, ice, and ecosystems, and are integrated to project the climate of a particular region or domain.
190 In this research, we use the sixth generation of the Canadian regional climate model (CRCM6/GEM5.0),
191 which is currently under development at the Centre pour l'Étude et le Simulation du Climat à l'Échelle
192 Régional (ESCER) of the University of Quebec at Montréal (UQAM). Two studies have recently evaluated
193 the performance of this newly developed model in North America (Moreno-Ibáñez and others, 2023; Roberge
194 and others, 2024). The version of CRCM6/GEM5.0 used in this study is based on version 5.0.2 of the
195 Global Environmental Multiscale Model (GEM5) (McTaggart-Cowan and others, 2019; Girard and others,
196 2014), which serves as the operational numerical weather prediction model for the Meteorological Service
197 of Canada. The CRCM6 model uses a 12 km (0.11°) spatial grid based on the Regional Deterministic
198 Prediction System (RDPS) configuration of the 5.0.2 version of the Global Environmental Multiscale model
199 (GEM5) (McTaggart-Cowan and others, 2019; Girard and others, 2014). This model was chosen for its
200 spatial downscaling capabilities and hourly time step, which we selected from 1982 to 2022.

201 To increase the overall representativeness of the modeled data, four grid points were selected around
202 the coordinates of the CAELA weather station and the mean value was extracted. The data were provided
203 and processed by the ESCER. The mean elevation of the four grid points is 679 m, which represents a
204 slight overestimation of the actual weather station, which is at 630 m. Previously, Imbach and others
205 (2024) observed an underestimation of snowfall and snow height in the CRCM6 dataset for the CAELA
206 weather station study site. The underestimation was rate dependent, and the underestimation was greater
207 at higher snow rate precipitation. Their precipitation bias assessment analysis and correction was used to
208 positively correct the observed underestimation. The correction made was based on the correction made
209 at Rogers Pass, Western Canada by (Bellaire and others, 2011). Furthermore, a statistical validation of
210 the CRCM6 against *in-situ* recorded data showed an overall strong representativeness. Their correction
211 was applied to the snow precipitation and snow depth of the CRCM6 outputs.

212 Meteorological data from other locations

213 To compare our data with potentially similar locations around the globe and existing snow climate classi-
214 fication, we adapted the boxplot figure from Mock and Birkeland (2000), incorporating each of the climate
215 indicators to visually compare the mentioned regions. We also used data directly from the snow study of
216 Ikeda and others (2009) for the Central Japanese Alps, and data from Mt. Washington in New Hampshire,
217 USA (Meloche, 2019), which is also similar to the Chic-Chocs.

218 Snow cover modeling

219 The snow cover model SNOWPACK is a multilayer one-dimensional thermodynamic model and was used
220 to simulate the snow cover stratigraphy and properties for each snow season (Lehning and others, 1999).
221 The required meteorological data input were driven from the CRCM6 model, which were air temperature,
222 relative humidity, wind speed and direction, short and long wave radiation (incoming and outgoing), total
223 precipitation, and snow height. In this study, SNOWPACK was run using hourly CRMC6 data with
224 snow height forcing. The model parameters were based on previous work and validation performed by
225 members of the research team for the same study area (Côté and others, 2017) and also in western Canada
226 (Madore and others, 2018, 2022). We chose to use the default SNOWPACK snow/rain threshold of 1.2
227 °C, and the main parameterizations (SNOWPACK parameters) used were the BELLAIRE snow density
228 parameterization, the MONTI hardness parameterization, the Bucket water percolation model, and the

229 MO-MICHLMAYR atmospheric stability . The snow height in the simulation was enforced with the snow
230 height predicted by the CRCM6 model, with the corrected precipitation of Imbach and others (2024). The
231 snow cover was simulated every hour from October 1 to May 31, on the flat and also on two 38° virtual
232 slopes on a northern and southern aspect.

233 **Snow grain type**

234 The seasonal snow grain type distribution was computed from the snow cover model output by adding the
235 thickness of each layer to a snow grain type class such as precipitation particles (PP), melt forms (MF),
236 or faceted crystals (FC). This process is repeated daily from December 1 to March 31. The frequency
237 distribution is normalized by the sum of all layer thicknesses for both north and south virtual slope during
238 the winter from December to March.

239 In order to assess the validity of the snow grain type obtained from the snow cover model, we compared
240 it from the snow grain type frequency retrieved from snow profile observations made by the Avalanche
241 Québec, which is responsible for avalanche forecasting in the Chic-Chocs region, for the winter of 2015
242 to 2018 (Meloche, 2019). The snow profiles were made at different aspects and elevations throughout the
243 region, with approximately 25 snow profiles per winter.

244 **Avalanche problem type**

245 *Weak layer identification*

246 The avalanche problem type was derived from the output of the SNOWPACK model i.e., from both, north
247 and south-facing slope simulations, following the methodology proposed by Reuter and others (2022). The
248 following section describes the general procedure of the method, for more details please refer to the original
249 paper. This method evaluates potential persistent and non-persistent instabilities on each day, which
250 could be either prone to natural release or artificial triggering. For the purpose of this study, only natural
251 release was considered. The non-persistent weak layer is composed of either precipitation particles (PP),
252 decomposed and fragmented particles (DF), and faceted rounded grains (FCxr). The persistent weak layers
253 are composed of faceted crystals (FC - FCxr), surface hoar crystals (SH) and depth hoar crystals (DH).

If a potential weak layer was present the day before or potentially buried, the properties of the slab
overlying this potential weak layer is judged. A minimum slab thickness of 0.18 m and a slab density of at
least 100 kg m⁻³ are required for a critical slab-weak layer combination (Reuter and others, 2022). Four

indices were then used to classify all potential slab-weak layer combinations in view of natural release. The S_N (natural) index was computed for each layer within the snowpack, defined by a ratio of the gravitational shear stress τ_g induced by the weight of the overlying slab and the shear strength of the weak layer:

$$S_N = \frac{\tau_g}{\tau_p}, \quad (1)$$

where $\tau_g = \rho gh \sin \psi$ is defined by the slab density ρ , the gravitational acceleration g , the slab height h , and the slope angle ψ . The time to failure t_f was also used to determine the natural stability of the layers, developed by Conway and Wilbour (1999). The time to failure is the time derivative of S_N :

$$t_f = \frac{S_N(t) - 1}{\frac{dS_N}{dt}}. \quad (2)$$

A second stability indicator is the critical crack propagation length a_c , which is the length required for crack propagation to begin. (Richter and others, 2019) proposed a method to derive the critical crack length from the SNOWPACK simulation based on stress and strength approach (Gaume and others, 2017) instead of using the weak layer fracture energy (Heierli and others, 2008). The method was also adapted with an empirically fitted F_{wl} parameter to improve the predictive performance with the SNOWPACK model. The critical crack length was calculated using the following expression, which was coded in the SNOWPACK module from Gaume and others (2017):

$$a_c = \Lambda \left[\frac{-\tau + \sqrt{\tau + 2\sigma(\tau_p - \tau)}}{\sigma} \right], \quad (3)$$

where $\sigma = \rho g D \cos \psi$ and λ is a characteristic length of the system defined by:

$$\Lambda = \sqrt{E' D F_{wl}}, \quad (4)$$

254 where $E' = E/(1 - v^2)$, v is the Poisson ratio set to 0.3, F_{wl} is the fitted parameter developed by Richter
 255 and others (2019). All two stability indices S_N and a_c mentioned above are already available as output
 256 variables in the SNOWPACK code (v3.6). The time to failure t_f was coded in Python based on the time
 257 derivative of S_N .

258 Based on these three indices, we classified each potential layer as an unstable weak layer using the
 259 thresholds determined by Reuter and others (2022). A weak layer was classified as critical for natural

260 release if $S_N < 3.6$ and $t_f < 18$ h, and $a_c < 0.32$ m. Then, for each unstable weak layer, we classified it as
261 a persistent or non-persistent weak layer depending on the weak layer grain type. The snow grain types
262 of each critical weak layer were counted to get a frequency of weak layer snow grain type of the simulated
263 40-year period.

264 *Assigning Avalanche problem*

265 The following avalanche problem types were derived from the SNOWPACK model output: new snow
266 (NAP), wind slab (WSAP), persistent (PAP), and wet (WAP), based on the methodology developed by
267 Reuter and others (2022). On each day, after classifying the critical persistent and non-persistent weak
268 layers, we look at the concurrent snow load modeled in SNOWPACK. A non-persistent weak layer within
269 a 24-hour snowfall (HN24) greater than 5 cm is classified as a new snow problem (NAP). If a persistent
270 critical weak layer is loaded by a precipitation rate greater than 0.05 m/24h, the algorithm will classify it
271 as a persistent avalanche problem (PAP) and a new snow avalanche problem (NAP). The same procedure
272 is used for a wind slab avalanche problem (WSAP) with a 24h wind transport (`wind_trans24`) greater
273 than 0.4 m/24h and a non-persistent weak layer. A WSAP is also possible if the `wind_trans24` is above
274 the threshold and soft snow is present on the surface within three days. The algorithm will classify both
275 a PAP and WSAP when the wind transport threshold is reached with an unstable persistent weak layer.

276 The assessment of the wet-snow avalanche problem is based on the liquid water content index developed
277 by Mitterer and Schweizer (2013) along with the number of days since isothermal conditions were reached
278 (Baggi and Schweizer, 2009). This index measures the liquid water per snow volume for each SNOWPACK
279 layer, with an averaging process that considers the thickness of these layers to determine the total liquid
280 water content of the snow cover. The index compares the total water content of the snow cover to a critical
281 threshold of 1% water by ice volume (Mitterer and others, 2016). A liquid water content index of 1 indicates
282 the onset of natural wet-snow avalanches, then, the snow cover returns to a stable state after four days of
283 sustained isothermal conditions (Baggi and Schweizer, 2009). We assign the avalanche problem for both the
284 virtual north and south face slope of every winter of the 40-year period. We used the `find_aps.py` function
285 to find all avalanche problem types from the SNOWPACK outputs based on the methodology of Reuter
286 and others (2022), in AVAPRO available in the package the *snowpacktools* from the public repository of
287 the Avalanche Warning Service Operational Meteo Environment AWSOME (AWSOME Core Team, 2024).

288 In order to assess the validity of the avalanche problem type derived from the SNOWPACK modeling,

289 we compared it with the forecasted avalanche problem type from Avalanche Québec for the winter of
290 2012 to 2018 (Meloche, 2019). The predicted avalanche problem types are the forecaster's assessment for
291 the upcoming forecast period based on meteorological observations, snow cover observations, and weather
292 forecasts. The forecast period was two days for winters 2013 to 2015 and daily for winters 2016 to 2018.

293 **Clustering**

294 Finally, we performed a k-means cluster analysis to explore a different classification of the avalanche
295 characteristics of the study area. The k-means is a clustering analysis that uses the proximity to a geometric
296 position in the feature coordinate space (Macqueen, 1967). The k-means was run with data from 40 winters,
297 including north- and south-facing slope simulations for the avalanche problem type. We neglected the
298 climate indicators and the snow grain type to reduce dimensionality and to replicate the same method as
299 Reuter and others (2023). In addition, the avalanche problem type integrates the weather context and snow
300 grain type from the critical weak layer. To select the ideal number of clusters, we computed the silhouette
301 score and the Calinski-Harabasz score for clusters ranging from 2 to 10. We selected the number of clusters
302 with the maximum values of Silhouette score per number of cluster, and Calinski-Harabasz score. The
303 number of clusters when one of the individual clusters were below the average score was not considered.
304 We also performed principal component analysis on the dataset to explore linearity between variables and
305 to ease visualization of our clustering results. The result of the clustering analysis will be compared to the
306 French alps where a similar analysis is available for comparison Reuter and others (2023).

307 **RESULTS**

308 **Snow Climate classification**

309 *10 years of meteorological data*

310 As a first result, we present 10 years (2013-2022) of meteorological data recorded at the Mt Ernest-Laforce
311 weather station and data simulated by the climate model CRCM6. The Chic-Chocs study areas generally
312 exhibited cold average winter temperatures (meanTA < -7°C) and limited total winter snow precipitation
313 (Snow < 450 mm SWE). The winters of 2016 and 2021 showed warmer conditions, but only the winter of
314 2021 showed significant rain during the winter season (Table 1). The winters of 2013 and 2020 were also
315 warmer, but less than 2016 and 2021, with a significant amount of Rain (67.8 and 77.0 mm, respectively).

Table 1. Results of the Mock and Birkeland (2000) classification with weather station Mt Ernest-Laforce and the CRCM6 climate model. The year in the column winter represent the month of January, indicating that the winter of the present year includes December of the prior year.

Winter	Rain (mm)		meanTA ($^{\circ}\text{C}$)		meanDEC ($^{\circ}\text{C m}^{-1}$)		SWE (mm)		Snow (cm)	
	CAELA	CRCM6	CAELA	CRCM6	CAELA	CRCM6	CAELA	CRCM6	CAELA	CRCM6
2013	67.8	117.6	-10.0	-10.5	16.2	19.1	489.4	470.1	713.8	328.8
2014	6.0	15.5	-13.8	-15.3	13.7	35.0	474.4	465.8	689.3	318.8
2015	48.0	34.1	-14.7	-14.5	13.7	11.8	426.4	425.5	446.7	277.8
2016	42.3	37.6	-9.5	-10.7	NA	29.1	422.3	453.4	NA	314.9
2017	15.7	36.8	-11.0	-12.4	21.7	27.5	475.9	516.6	725.1	374.3
2018	50.7	37.4	-10.7	-12.4	17.9	19.7	405.6	491.9	516.6	368.2
2019	15.5	52.0	-12.6	-14.0	19.1	17.7	211.4	512.8	493.6	341.6
2020	77.0	54.6	-10.7	-12.1	13.1	18.4	444.3	441.2	437.0	303.7
2021	93.6	106.1	-8.6	-9.7	16.1	22.3	502.3	425.3	546.4	339.3
2022	15.7	43.7	-12.2	-13.3	10.9	16.5	509.4	570.0	535.4	419.4

316 The meanTA fell below -7°C , and the meanDEC was consistently above $10^{\circ}\text{C m}^{-1}$. This combination
 317 of cold mean air temperatures and sparse snow cover likely contributed to the pronounced temperature
 318 gradients observed (Table 1).

319 Figure 2 shows the difference between the CAELA weather station and the CRCM6 model. The SWE
 320 estimation with the CRCM6 model are good with the exception of the winter of 2019. We suspected
 321 a problem with the precipitation gauge during this winter, so the error may not be from the CRCM6
 322 model. However, despite the precipitation correction and snow height forcing in SNOWPACK, the snow
 323 height (Hs) and snowfall were underestimated by the CRCM6 model. Figure 2 shows that the CRCM6
 324 model simulated colder temperatures compared to the weather observations. However, this colder bias did
 325 not translate into a systematic underestimation of precipitation, which has no clear systematic bias with
 326 some winters precipitation being underestimated and others overestimated. Finally, the mean December
 327 temperature gradient was slightly overestimated by CRCM6 with less snow height.

328 The results of the snow climate classification derived from Mock and Birkeland (2000) flowchart in-
 329 dicated a predominantly continental climate for 8 winters over 10, and maritime classification for the
 330 remaining two winters (Table 1). The winter 2013 had a continental classification at the weather station,
 331 but a maritime classification with the CRCM6 model. The key determinant in classifying most winter sea-

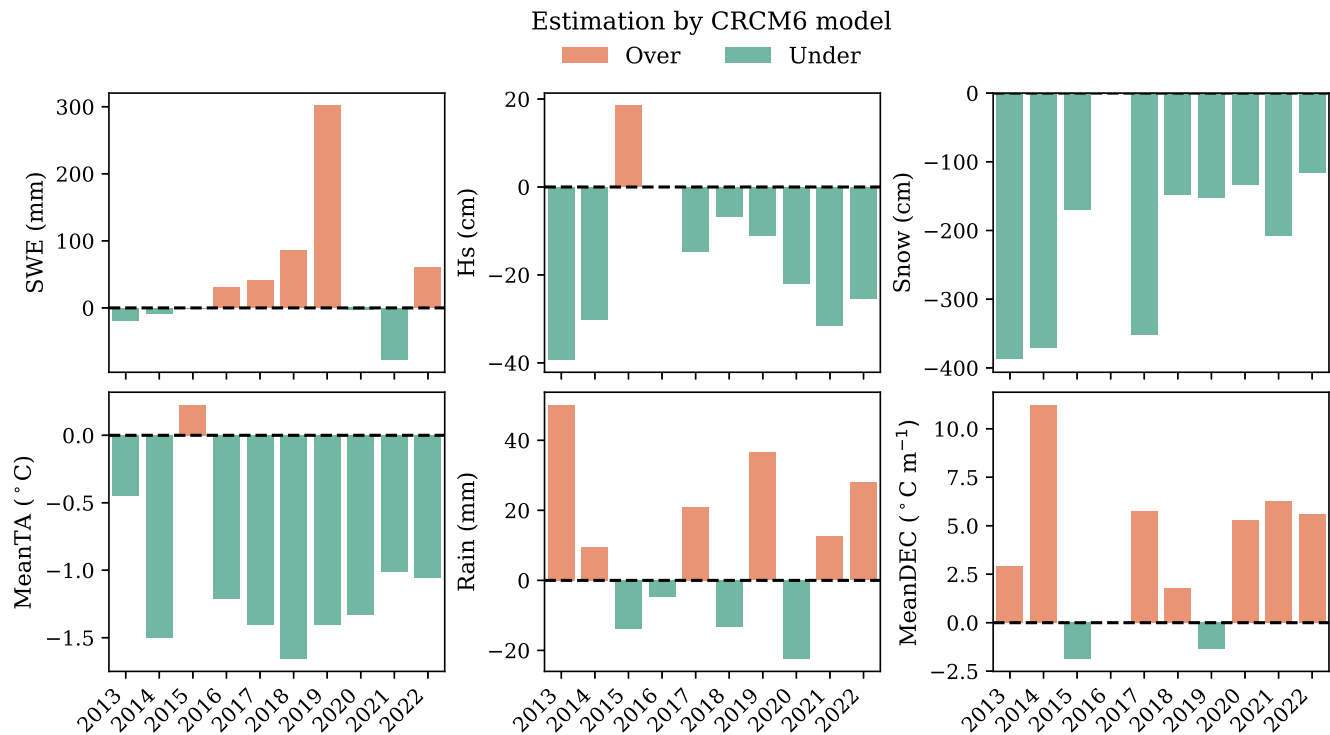


Fig. 2. Estimation of the climatic indicators used in Mock and Birkeland (2000) algorithm by the CRCM6 model, except for the snow height H_s . The estimation is compared to the weather observations at the CAELA station. The positive difference represents an overestimation (orange) of the CRCM6 model, and the negative difference represents an underestimation (blue) of the CRCM6 model.

332 sons was the mean December temperature gradient (meanDEC), which exceeded $10^{\circ}\text{C}/\text{m}$ for a continental
 333 climate and rain amounts exceeding 80 mm for a maritime climate (Table 1). The algorithm never met
 334 the "snow accumulation" criterion for classification into maritime and transitional snow climates during
 335 the classification process for both weather data (weather station and CRCM6).

336 40 years snow climate classification

337 Figure 3 shows a time series of the rain and mean air temperature for the last 40-winter simulations from
 338 the CRCM6 model. The classification results is also shown by the background color for each year where
 339 blue is for continental and red for maritime, as the transitional snow climate was never classified for the 40
 340 winters. The rain indicator was the only indicator that classified some winter as maritime (above the dashed
 341 line in Figure 3). Most of the winters (33/40) were classified as continental based on the mean December
 342 temperature (meanDEC). The mean air temperature is relatively cold and never exceeds -8°C , which is

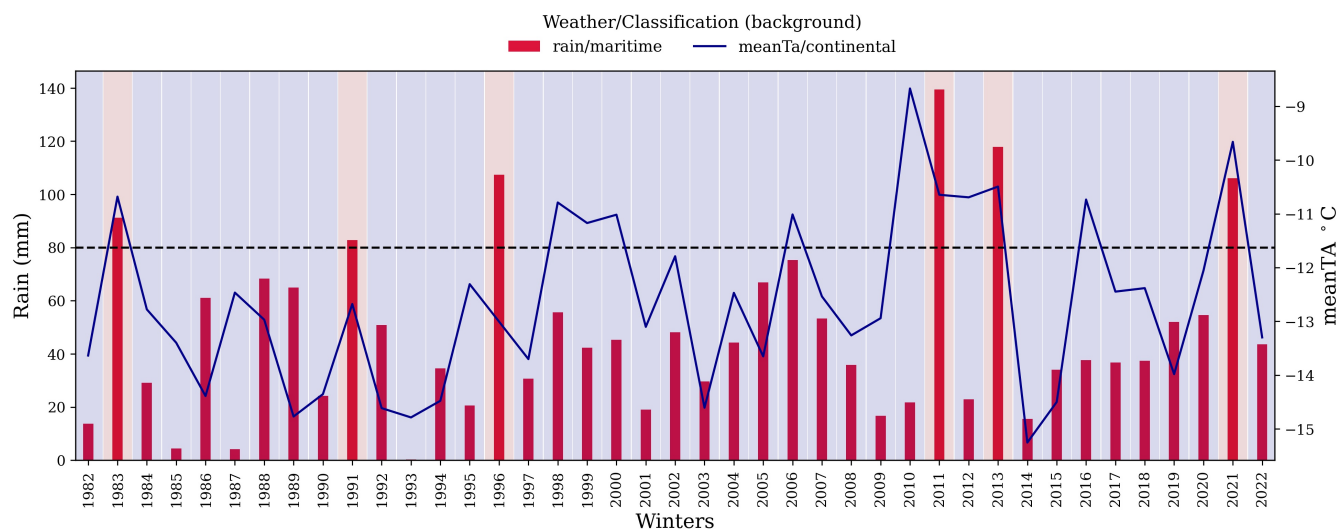


Fig. 3. Time series of the mean air temperature and total rain for the winter 1982 to 2022. The result of the Mock and Birkeland (2000) classification is shown with background color for each winter: the blue color is a continental classification, red is for maritime, transitional was never present). The mean air temperature is shown in dark blue and the total rain during the winter is shown in dark red. The black dashed line the 80 mm rain threshold for the maritime classification.

343 far from the -3°C threshold for a maritime winter. Some winters have been classified as maritime (7/40),
 344 and these winters are spread over the entire 40-year period. Despite the generally cold temperatures, rain
 345 events occur almost systematically every winter. Rain on snow event during the winter, combined with cold
 346 air temperature ($\text{meanTA} < -7^{\circ}\text{C}$) are the two main characteristics that define the region's snow climate.

347 *Global Comparison*

348 To compare our data with potentially similar locations around the globe, we adapted the boxplot figure from
 349 Mock and Birkeland (2000). First, we look at the two critical criteria used by the Mock and Birkeland (2000)
 350 algorithm for classification, which were meanDEC above $10^{\circ}\text{C m}^{-1}$ (continental) and Rain above 80 mm
 351 (maritime) (Mock and Birkeland, 2000). These two criteria were in similar ranges to those for the Chic-
 352 Chocs, Central Japan, and Mt. Washington (Figure 4). The SWE, snowfall, and December temperature
 353 gradient for Central Japan were more comparable to the Chic-Chocs. The amount of precipitation was
 354 similar in all areas: Chic-Chocs, Central Japan, and Mt. Washington (Figure 4). We also compared all
 355 three areas to the three classic snow climates of the western United States (Mock and Birkeland, 2000).
 356 Snow-related parameters such as SWE, snow depth, and December temperature gradient were within the

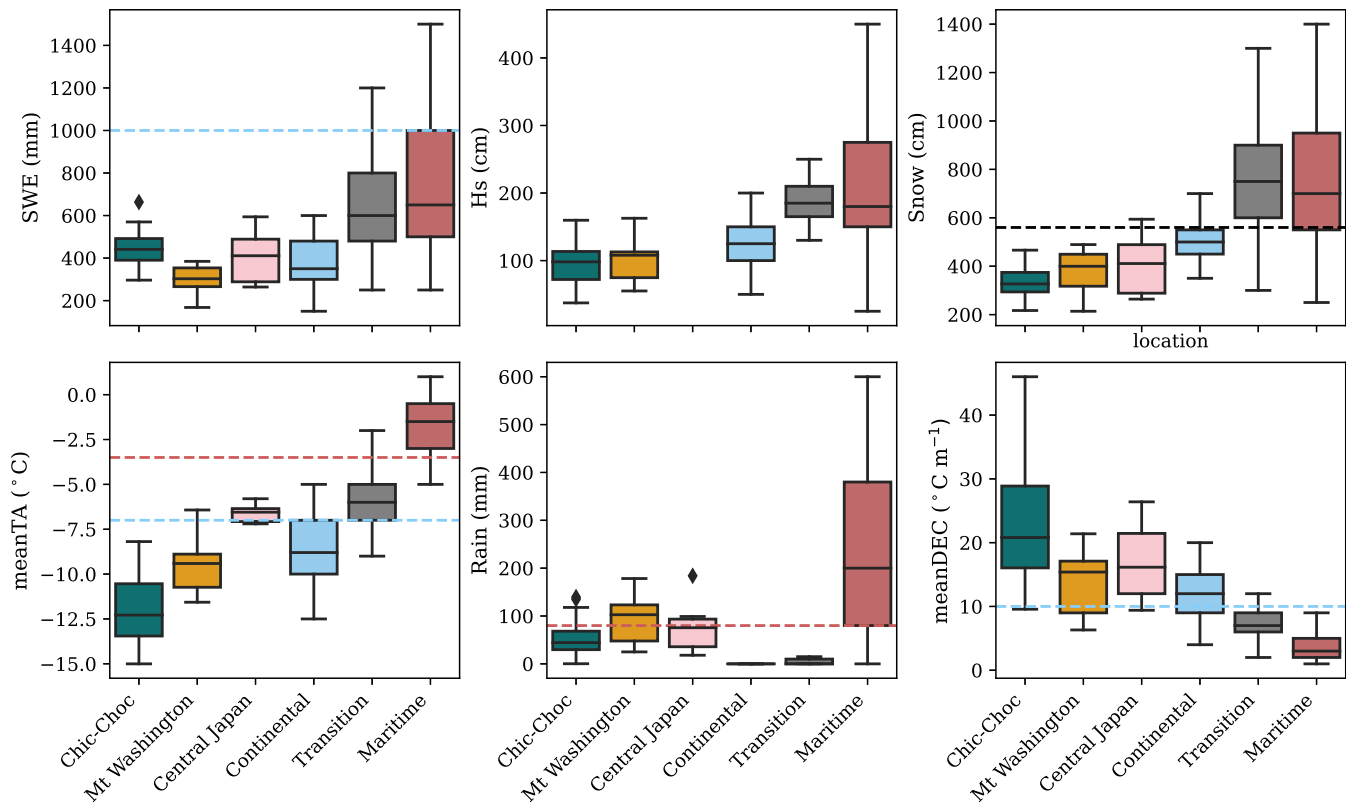


Fig. 4. Box plot with all the Mock and Birkeland (2000) climate classification for a global comparison with the Chic-Chocs dataset, Mt Washington from Meloche (2019), Central Japan from Ikeda and others (2009).

357 range for a continental snow climate (Figure 4). Air temperature was also within the range for a continental
 358 climate, with the Chic-Chocs and Mt. Washington at the colder end and Central Japan at the warmer end
 359 (Figure 4). Precipitation was the only determinant that fell within the Maritime snow climate range for
 360 all regions. These results indicate that all regions, Chic-Chocs, Mt. Washington, and Central Japan, were
 361 similar to the continental snow climate, except for precipitation, where they were similar to a maritime
 362 snow climate (Figure 4).

363 Snow grain type

364 We compared the frequency of the grain types simulated in SNOWPACK using CRCM6 model with snow
 365 profile observations from 2015 to 2018. Figure 5 shows a systematic discrepancy between observations
 366 and the simulated data. SNOWPACK tends to simulate melt forms (MF) more frequently than they
 367 are observed. Conversely, the simulation results seem to under-represent decomposing and fragmented
 368 particles (DF). The presence of rounded grains (RG) and precipitation particles (PP) is similar between

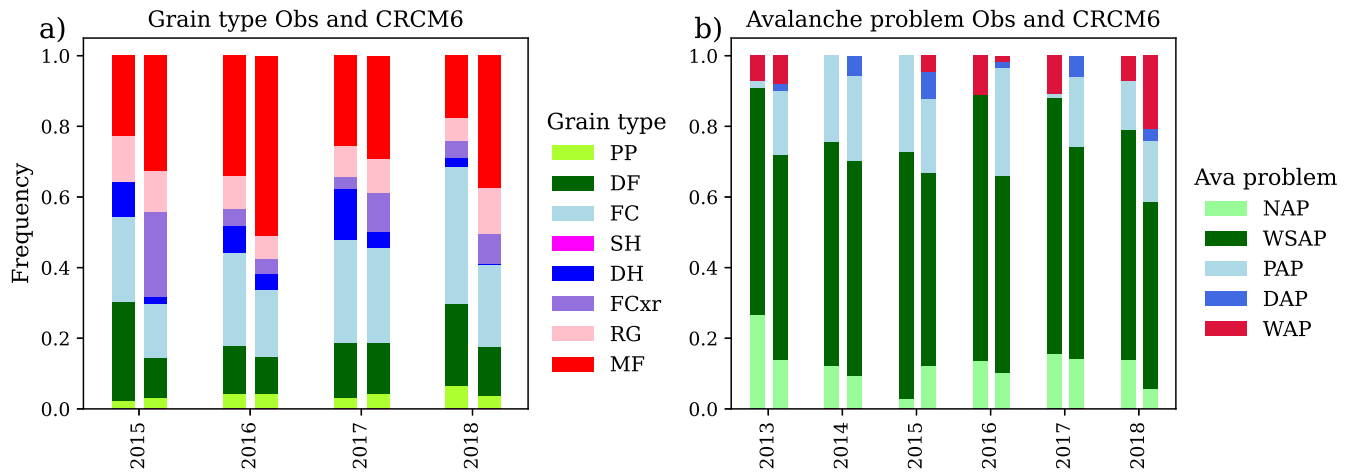


Fig. 5. Comparison of the observations vs the simulated (CRCM6/SNOWPACK) for a) snow grain type distribution, and b) Avalanche problem frequency. The left barplot is the observations from Avalanche Québec and the right barplot is the climate simulation CRCM6 dataset. The avalanche problem type are the following : New snow avalanche problem (NAP), wind slab avalanche problem (WSAP), persistent avalanche problem (PAP), Deep persistent avalanche problem (DAP), and wet avalanche problem (WAP).

369 the simulation from the model chain CRCM6/SNOWPACK and the observations. The faceted crystals
 370 (FC) are more often observed in the snow profiles, but the faceted rounded grains (FCxr) are more frequent
 371 in the simulation from the model chain CRCM6/SNOWPACK. However, these grain types are similar and
 372 represent a similar transformation process in the snow cover. Finally, depth hoar (DH) was more frequent
 373 in the snow profiles. Despite the small difference between the simulations and the observations, the model
 374 chain CRCM6/SNOWPACK is relevant to retrieve the seasonal snow grain type distribution.

375 The snow grain type distribution was retrieved from the 40-year SNOWPACK model to get an overview
 376 of the temporal variability in metamorphic process of the study area. First, the snow grain type shows that
 377 melt forms (MF) are predominant in the snow cover from December to the end of March (Figure 6-a). The
 378 second most frequent grain type are rounding faceted grains (FC). However, Figure 6-a shows that there is
 379 a temporal variability between winters, with some winters having more FC than MF. The third and fourth
 380 most abundant grain types were faceted crystals (FCxr) and rounded grains (RG). The presence of these
 381 two grain types was quite variable between winters, sometimes with more FCxr than RG and sometimes
 382 vice versa (Figure 6-a). Surface hoar was not present in the snow cover during the entire 40-year period.
 383 Overall, the 40-years of seasonal grain type distribution demonstrated different dominant metamorphic
 384 processes that should impact the dominance of specific avalanche problem types (i.e. persistent vs wet

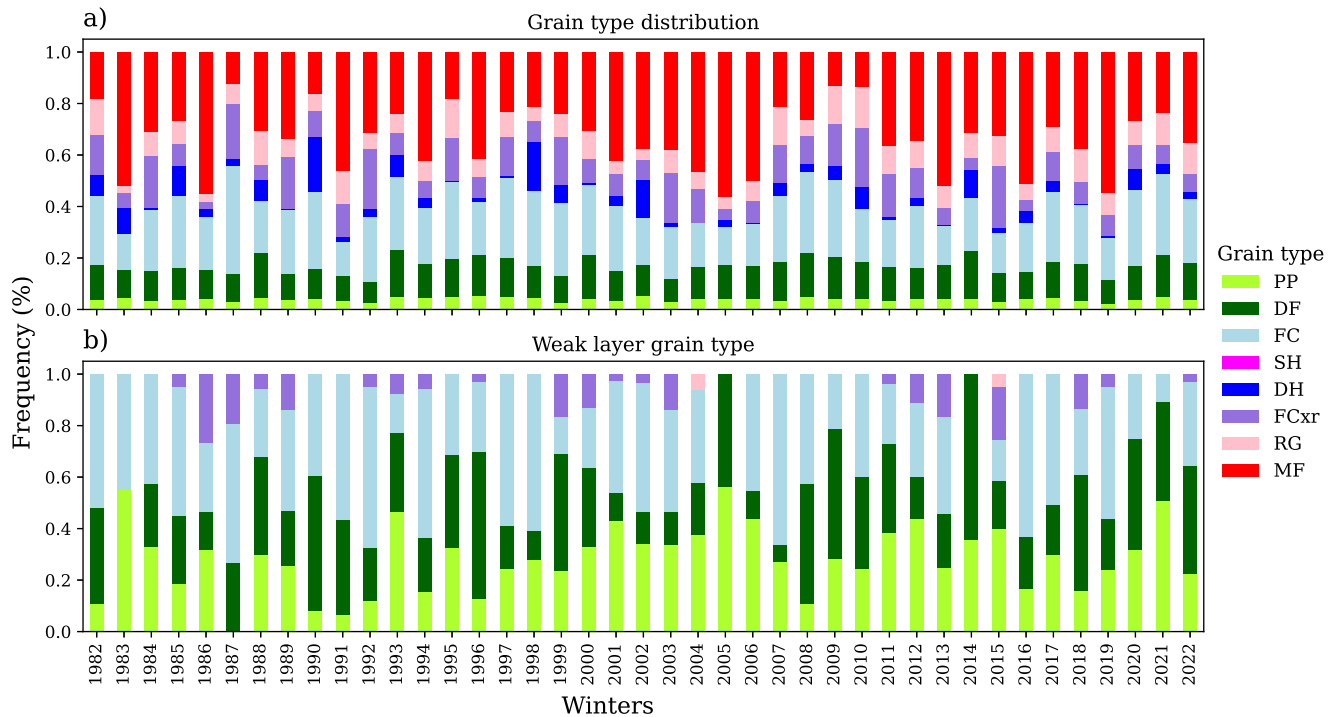


Fig. 6. Snow grain type distribution over the 40 winters period with a) snow grain type distribution of the whole snow cover each winter from December to the end of March, and b) the snow grain type distribution of the weak layer assessment for each winter (natural instability).

385 avalanche problem type).

386 The snow grain type distributions are different if looking at critical weak layers from the avalanche
 387 problem assessment (Figure 6-b). The three most common weak layer grain types are precipitation particles
 388 (PP), decomposing and fragmented particles (DF), and faceted crystals (FC). Like the overall grain type
 389 assessment, the most frequent weak layer grain type was not the same from winter to winter, where
 390 sometimes DF and PP were more frequent over FC, and some other winters the opposite occurs where
 391 FC was more frequent. It is important to note that this assessment is based on a weak layer with natural
 392 instabilities, and the frequency might change with including skier triggering. Some winters also had the
 393 FCxr in the weak layer assessment and two winters had few weak layers with RG as grain type. It is
 394 important to note that during the simulated 40-year period neither DH nor SH were present in the critical
 395 weak layers.

396 To explore the "typical" stratigraphy of the study area, two examples of simulated snow profiles (38
 397 ° north facing slope) for Maritime and Continental winters are presented in Figure 7. The 'continental'
 398 winter of 2018 included a large rain event on 13 January (35 mm), which initiated a wet instability cycle

399 for the next 10 days (Figure 7-a). After this event, however, colder conditions returned, with snow depths
400 continuing to increase with several layers of FC, up to a maximum snow depth of 240 cm. These cold
401 conditions persisted until the end of March. The "maritime" winter of 2021 had a large rain event (25
402 mm), which occurred on 25 December with a thinner snow cover (43 cm) and caused the snow cover to
403 melt almost completely (Figure 7-b). The rain event delayed snow accumulation, resulting in a shallower
404 snow cover compared to the continental winter of 2018. Despite the difference in amount and timing of
405 the rain event in both winters, the resulting stratigraphy was quite similar and more representative of a
406 continental snow cover with a thick melt-freeze crust in the basal layers, with FC above and DF/PP at
407 the surface. The rains at the end of March were the main cause of this so-called maritime winter. This
408 sequence of meteorological and different layers leads to a specific type of avalanche problem during the
409 winter. In the following section, the winters of 2018 and 2021 are described in more detail in terms of
410 avalanche problem type.

411 **Avalanche problem type**

412 *Continental vs Maritime winter*

413 Figure 7 shows the timing of avalanche problem types during the continental winter of 2018 and the
414 maritime winter of 2021. The continental winter of 2018 had more natural instabilities compared to the
415 maritime winter of 2021, with more significant storms producing more NAP, WSAP, PAP and DAP. The
416 persistent problems (PAP/DAP) were more concentrated at the beginning of the winter, and the rain
417 event of 13 January had removed the persistent weak layers. Surprisingly, the continental winter had
418 more wet-snow instabilities (WAP) despite having less total rainfall during the winter (50 mm) compared
419 to the maritime winter (93 mm). The persistent problems were concentrated towards the end of the
420 winter in January, February and March. Regarding the avalanche problem type, the difference between
421 the "maritime" and the "continental" winter was not significant and does not correspond to the definition
422 of a maritime winter (more precipitation, less or no PAP/DAP).

423 *Observations vs Simulations*

424 We compared the seasonal frequency of predicted avalanche problem types from Avalanche Québec with
425 those derived from snow cover modeling. In both cases, the most common avalanche problem type was wind
426 slab avalanche problem (WSAP). Avalanche Québec generated slightly more WSAPs than the simulation

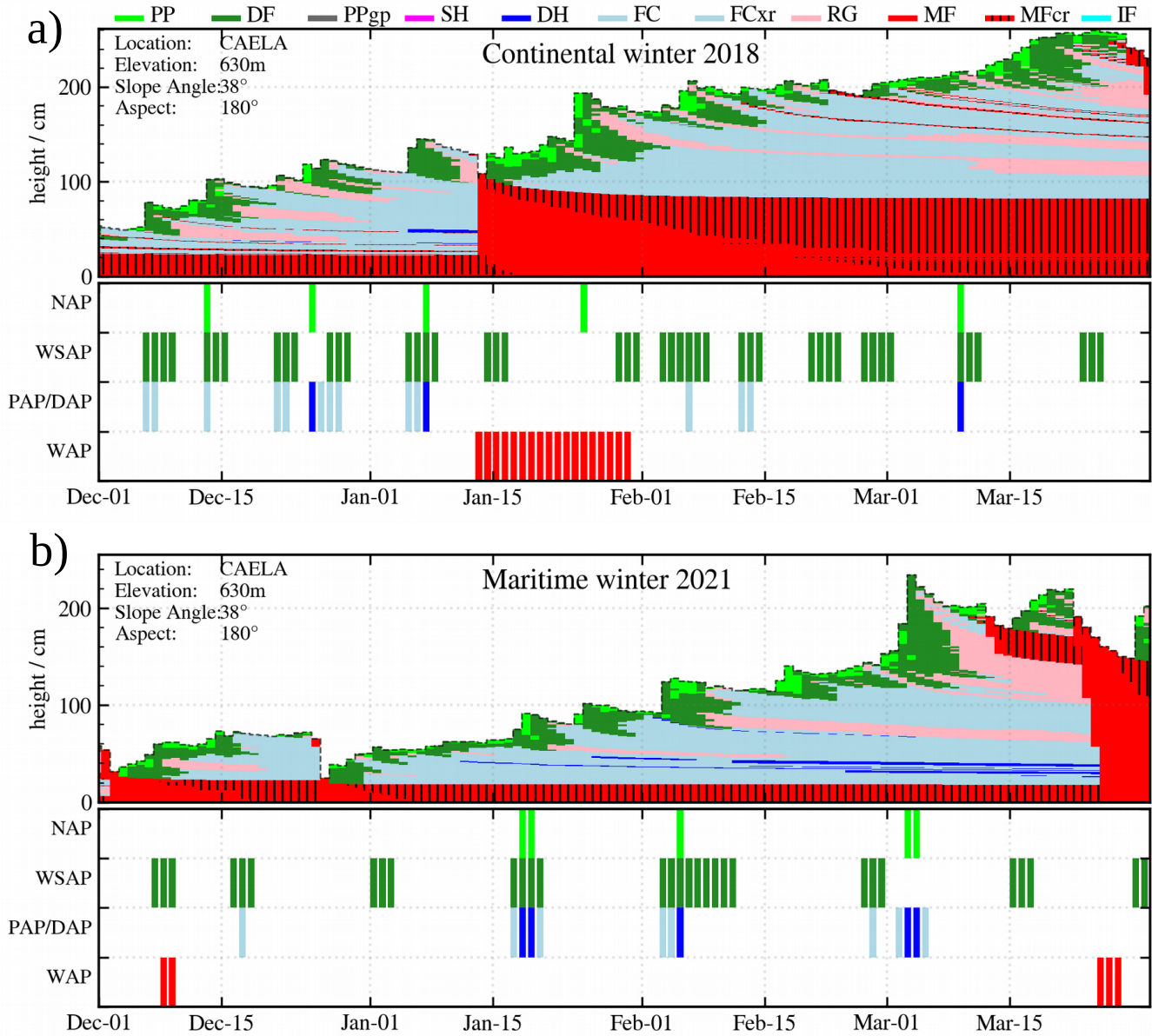


Fig. 7. Seasonal stratigraphy and avalanche problem type from the snow cover model output for a) an example Continental winter in 2018, and b) an example of a stratigraphy during the Maritime winter of 2021. New snow avalanche problem (NAP), wind slab avalanche problem (WSAP), persistent avalanche problem (PAP), Deep persistent avalanche problem (DAP), and wet avalanche problem (WAP).

427 from the CRCM6/SNOWPACK model chain. New snow problems (NAP) were more frequent compared
428 to the simulation expected for the winter of 2015. Conversely, the persistent problem type (PAP) was
429 also more frequent in the simulation compared to the Avalanche Québec forecast. Thus, NAP and WSAP
430 were underestimated and PAP/DAP were overestimated by the CRCM6/SNOWPACK model chain. The
431 winters of 2016 and 2017 were the most different between the simulation and the forecasts of Avalanche
432 Québec, with no PAP/DAP and WAP (Avalanche Québec) compared to more PAP/DAP and almost no
433 WAP (CRCM6/SNOWPACK). The (WAP) was the most variable between simulation and forecast. The
434 deep persistent problem type (DAP) was never forecast by Avalanche Québec. These results show the
435 systematic error or difference between the simulation and the forecast of the avalanche problem type, but
436 we have to keep in mind that the significant differences could be related to the difference between the
437 forecast guidelines (Avalanche Québec) and the numerical model (CRCM6/SNOWPACK).

438 **40-year period**

439 Figure 8-a shows the distribution of natural avalanche problem types that have occurred in our study area
440 over the last 40 years. Four different avalanche problem types were present in the region, with the wind
441 slab avalanche problem type (WSAP) being the most prevalent in the region. The second most frequent
442 problem type was the persistent problem type (PAP) with an average of 13 days per winter and the deep
443 persistent problem type (DAP) with an average of 3 days per winter. The wet avalanche problem type
444 (WAP) was not present every winter with an average of 3.5 days/winter on a virtual northern aspect and
445 4.1 days/winter on a virtual southern aspect (Figure 7). The less frequent problem type was the new snow
446 problem type with an average of 7 days per winter.

447 Figure 8-b shows anomaly over the 40-year period, with the colored background representing the clas-
448 sification by the Mock and Birkeland (2000) algorithm. The distribution of avalanche problems does not
449 seem to be different for the maritime winter. The winters of 1991, 2011, and 2018 had the most WAP
450 anomalies of the dataset, but the winters of 1991 and 2011 were classified as maritime and the winter
451 of 2018 was classified as continental. However, other maritime winters appear to be the same as other
452 continental winters without specific anomalies, such as winter (1996, 2013 and 2021) (Figure 8-b). These
453 results indicate a possible limitation of the Mock and Birkeland (2000) algorithm and that the frequency of
454 the seasonal avalanche problem type can give a different perspective on what could be a "maritime" winter.

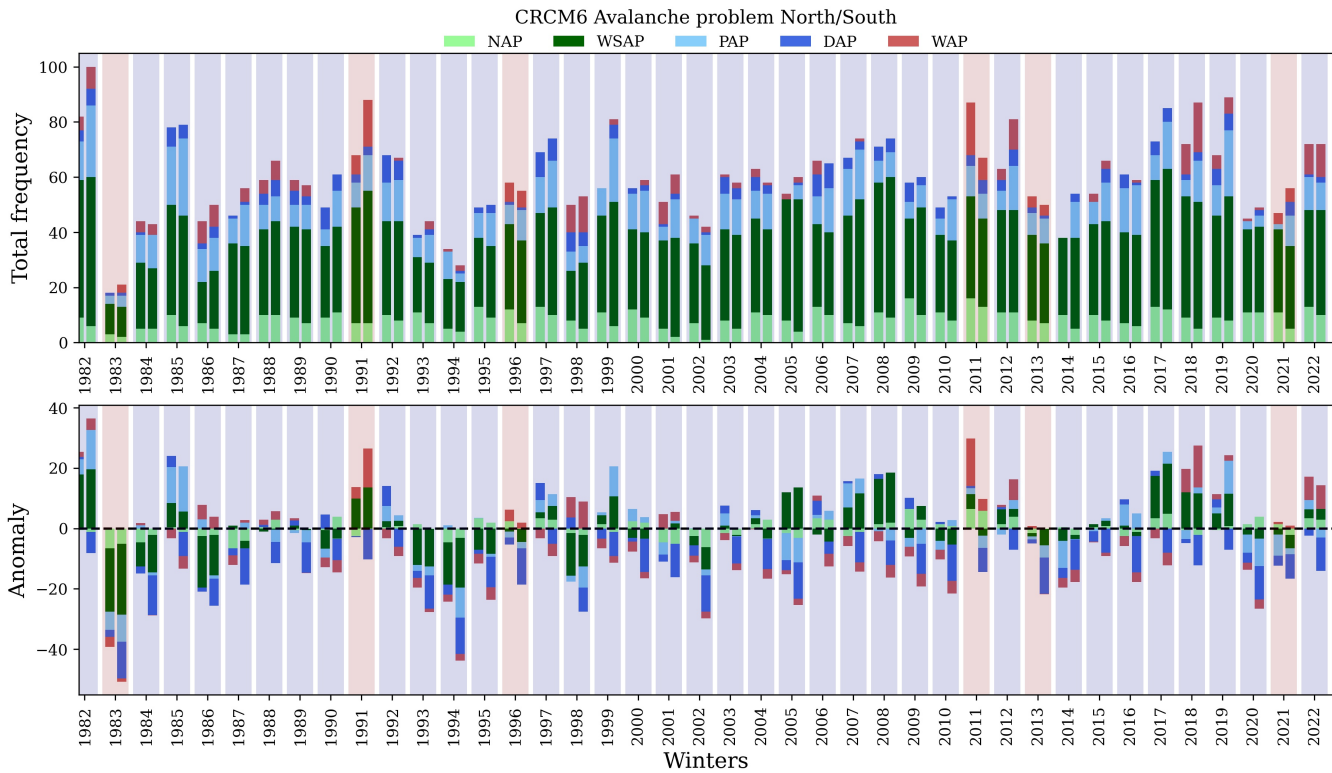


Fig. 8. Avalanche problem distribution for the winter 1982 to 2022, with the north face virtual slope on the left barplot and the south face on the right barplot. a) number of days where the problem type was issued, and b) the anomaly from the mean of the 40-year period. The blue colored background are winter classified as continental and the red is maritime. The avalanche problem type are the following : New snow avalanche problem (NAP), wind slab avalanche problem (WSAP), persistent avalanche problem (PAP), Deep persistent avalanche problem (DAP), and wet avalanche problem (WAP).

455 Clustering analysis

456 To get a new perspective on snow climate classification, we decide to look the clustering of the avalanche
457 problem types. The result of the silhouette analysis shows that two clusters were the most significant for
458 classifying the northern and southern simulation for the 40 winters, with an average silhouette score of
459 0.25 and a Calinski-Haraszbasz score of 27.3. In close second, three clusters were also significant, with a
460 silhouette score of 0.24 and a Calinski-Haraszbasz score of 25.9. The remaining number of clusters (4,5,6..10)
461 had decreasing Silhouette and Calinski-Haraszbasz scores. Figure 9 shows the two and three clusters on a
462 transformed dataset using Principal Component Analysis (PCA) to visually represent the clustering. The
463 two clusters can be compared to a maritime and continental winters of the Mock and Birkeland (2000)
464 algorithm. However, the seven maritime winters were in both cluster (2 in the blue and 5 in the red)
465 (Figure 9). According to the vector variables of the PCA in Figure 9-c, the red cluster was characterised
466 by more WAP and early WAP onset date (Decembre and January). By opposition, the blue cluster had
467 more instabilities with all dry avalanche problem types and a late WAP onset date in April or later. These
468 two clusters were quite different from the classic maritime/continental, with the blue cluster had more dry
469 avalanche problem (NAP,WSAP, PAP/DAP). The only major difference between north and south aspect
470 was that more NAP were simulated on northern aspect, and surprisingly, there was no significant difference
471 in WAP or WAP onset date between aspect.

472 The three clusters that resulted from the analysis are presented in Figure 9-bd). The first cluster (red)
473 was characterised by more WAP and early WAP onset date mostly in December. The second cluster (pink)
474 was characterised by lowest NAP, WSAP and PAP/DAP with early to mid WAP onset date (January).
475 The third cluster (turquoise) had the latest WAP onset date (April), and the lowest WAP. However, the
476 maximum and the minimum values presented were relative to our dataset.

477 To compare our clusters with an other region, we present in Figure 10 our three clusters compared
478 to the data of Reuter and others (2023), who cluster the avalanche problem type of the French alps. We
479 compared the three clusters centroids of this present study with the four centroids founded in the French
480 Alps. Two clusters had similar centroids between both studies, which were the pink clusters (cluster 1
481 and 5) and and the turquoise-green clusters (cluster 3 and 8) (Figure 10. The pink cluster in both studies
482 had mid-season WAP onset date around February with a relatively low number of days with a persistent
483 avalanche problem with 10 or less, and around 5 days of new snow problems, and the lowest days of wind
484 slab problem. This cluster was observed, in the study of Reuter and others (2023), in the front ranges of

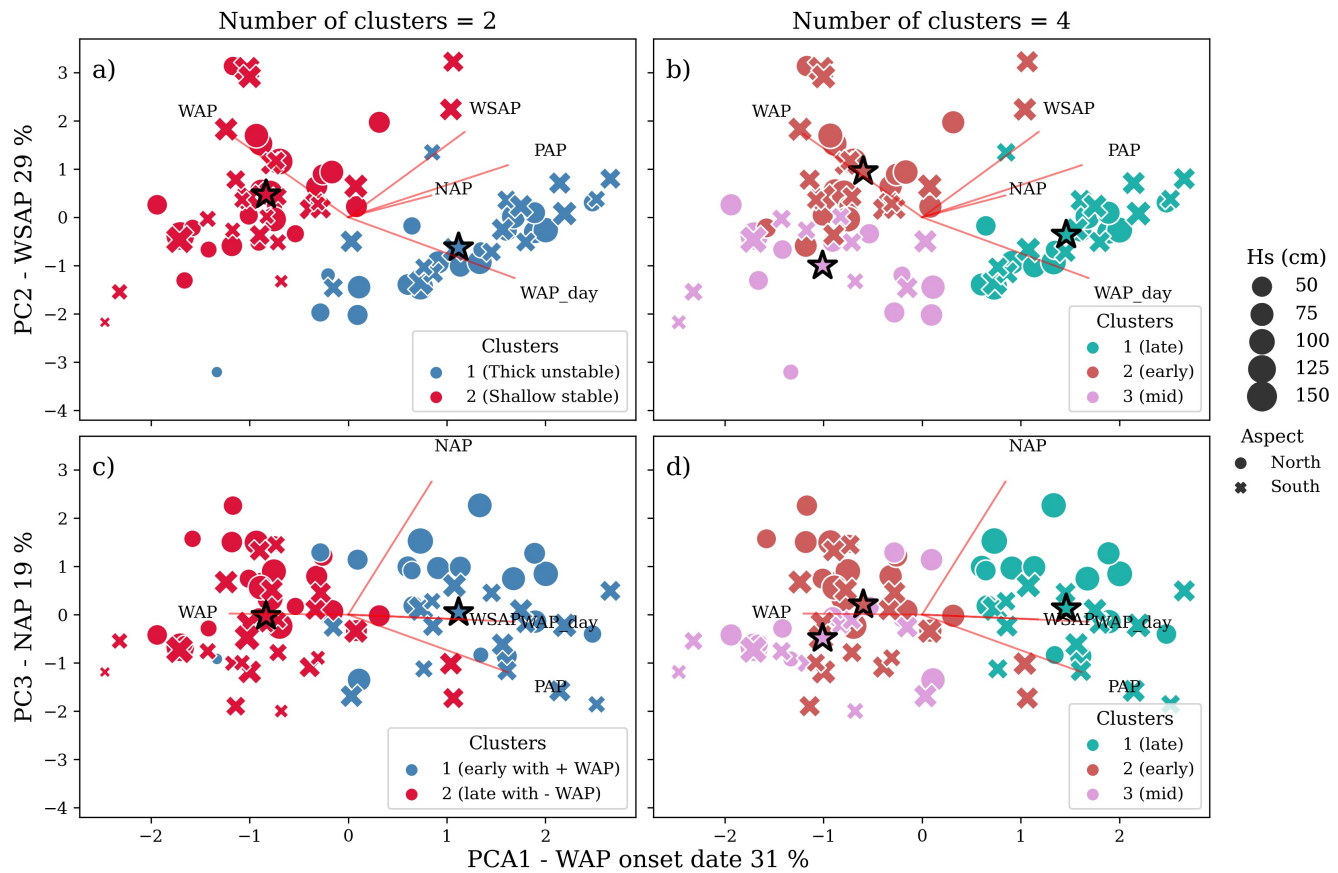


Fig. 9. K-means clustering with two and three clusters. The clusters are shown in relation to the principal component 1 (WAP onset date 31 %), principal component 2 (WSAP day 29 %), and the principal component 3 (NAP 19 %). The clustering with two clusters a) and c) demonstrates a new classification where winters were classified with a thick snow cover and unstable conditions, and other winters with shallow snow cover and stable conditions. The clustering with three clusters b) and d) demonstrates a different classification with snowy unstable winters, wet unstable winters and shallow snow cover and stable conditions.

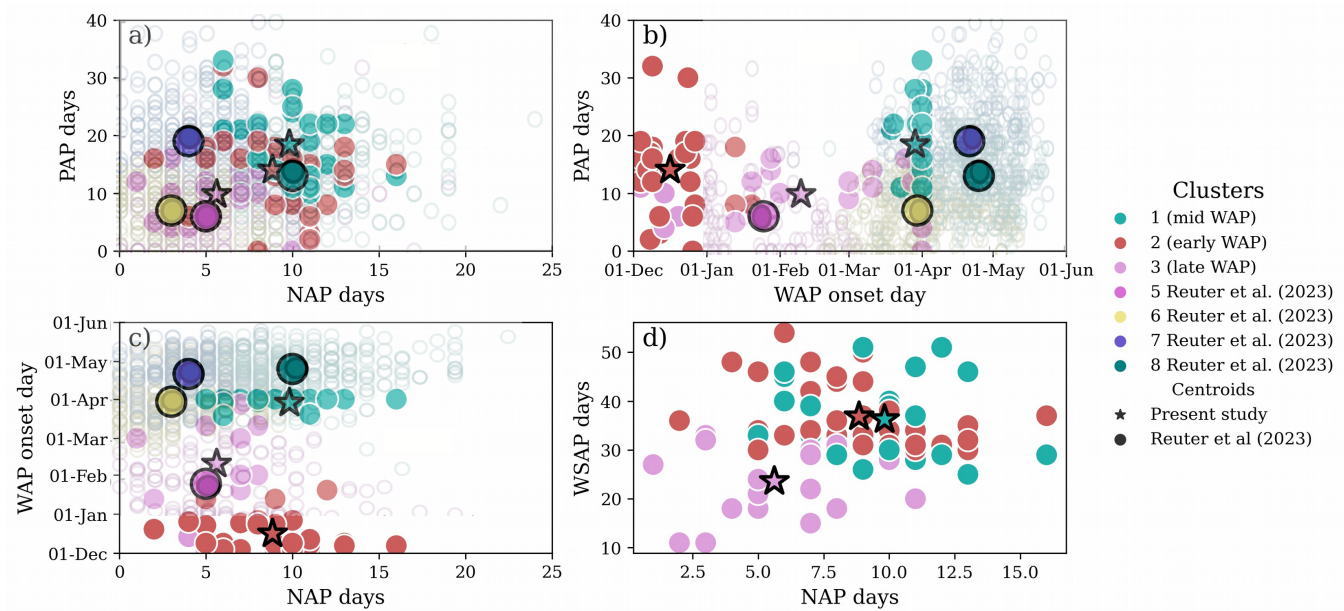


Fig. 10. Three clusters of this studies presented in comparison with the cluster centroids (cross) and the data in transparency of the study of Reuter and others (2023). The pink cluster of Reuter and others (2023) represents a cluster with low NAP, low PAP and a early WAP onset date before March. The green cluster of Reuter and others (2023) represents a cluster with high NAP, mid PAP and late WAP onset date after April. The yellow cluster of Reuter and others (2023) represents a cluster with high NAP, low PAP and mid WAP onset date around April. The purple cluster of Reuter and others (2023) represents a cluster with low NAP, high PAP and late WAP onset date around mid-April.

485 the French Alps, in regions like Vercors and Chartreuse, who classify mostly as "maritime" according to
 486 the Mock and Birkeland (2000) algorithm. The remaining cluster of this study (cluster 2 in red) does not
 487 fit with the other clusters from the Alps. Figure 10-bc shows the red cluster with a WAP onset date early
 488 during the season in December, which no cluster had such a early WAP onset date in the Alps. In terms of
 489 NAP and PAP days, the red cluster from our study was similar to the green cluster of Reuter and others
 490 (2023).

491 **DISCUSSION**492 **Can simulation data be used to classify snow climate?**

493 This research provides an in-depth analysis of the snow and avalanche climate of the Chic-Chocs region,
494 located in the northeastern Appalachian range in Canada. Through the use of climate indicators, snow grain
495 types, and avalanche problem types, we aim to provide a comprehensive understanding of snow processes
496 leading to avalanches in the region. Our dataset, derived from 40 years of CRCM6 climate simulation over
497 North America, serves as a robust basis for simulating snow stratigraphy and avalanche problem types over
498 this time period. This approach identifies snow cover characteristics relevant for avalanche situations. The
499 use of snow cover modeling provides a new perspective on snow and avalanche climates in the region and
500 complements the data available for snow and avalanche climatology.

501 Despite providing a significant temporal perspective, the model chain CRCM6-SNOWPACK simula-
502 tions we show have inherent uncertainties stemming from the climate data or the snow cover simulations.
503 To evaluate the performance of the CRCM6-SNOWPACK model chain, we present a comparison between
504 observations and the simulation for the climate indicators (Table 1), snow grain types (Figure 5-a), and
505 avalanche problem types (Figure 5-b). The uncertainties in the climate indicators and their classification,
506 as described by Mock and Birkeland (2000), are mainly due to the classification of precipitation as rain or
507 snow in both meteorological observations and CRCM6/SNOWPACK simulation. For example, the winter
508 of 2013 was classified as continental in the meteorological observations but as maritime using the CRCM6
509 simulations, highlighting the discrepancies between the observations and the simulations with respect to
510 precipitation events. Additional uncertainties arise from the precipitation gauge at the weather station,
511 where snow accumulation on top of the gauge can prevent accurate measurement during rain.

512 The SNOWPACK model, in the current settings used in this study, has limitations that could affect
513 the stratigraphy and thus the resulting uncertainty for avalanche problem types. As discussed in the
514 previous section, the classification between rain and snow is also a limitation of the threshold used in the
515 SNOWPACK model. We choose to use the default rain/snow threshold of 1.2 °C, which was empirically
516 determined based on measurements in Switzerland. Bellaire and Jamieson (2013) simulated the snow cover
517 in western Canada using numerical weather prediction of 15 km spatial grid, and tested different rain/snow
518 thresholds to detect melt-freeze crust formation in Rogers Pass, Canada. The default threshold of 1.2 °C
519 had the lowest probability of detection compared to other thresholds closer to 0 °C, which had a higher

520 probability of detecting melt-freeze crusts. However, Madore and others (2022) simulated the snow cover
521 in Roger Pass based on meteorological station and demonstrated that a threshold of 1.4 °C was better at
522 simulating both melt-freeze crusts while a accurate estimation of the snow height. They also point out
523 that this threshold was only found for the winter of 2018-2019, and that different winters could have a
524 different threshold based on a different meteorological event (i.e., thermal inversion) or even different snow
525 climate (Bellaire and Jamieson, 2013). This contrast between the results of Bellaire and Jamieson (2013)
526 and Madore and others (2022) supports the argument that this threshold could be different depending on
527 the meteorological context. Future work should focus on an effective way to find a adaptive rain threshold
528 to simulate melt event and melt-freeze layer.

529 The second limitation is related to a snow density problem in both CRCM6 and SNOWPACK. With
530 the correction of Imbach and others (2024), the estimation of SWE with average error of 54.5 mm, but with
531 an underestimation of snow height. The relatively good estimation of SWE but underestimation of snow
532 height could indicate a problem with the density of the new snow or the densification of the entire snow
533 cover. We used Bellaire's new snow density parameterization, which is an empirical fit of new snow density
534 based on several weather variables such as air temperature, wind speed, and relative humidity (Lehning and
535 others, 1999). This parameterization is an empirical fit based on measurements in Switzerland, but may
536 not be applicable in eastern Canada. Future work should investigate a different or new parameterization
537 of new snow density that is better suited to the snow climate of eastern Canada. Despite introducing
538 uncertainty in individual winter events, the CRCM6-SNOWPACK model chain was in good agreement at
539 representing the seasonal average of climatic indicators, snow grain type, and avalanche problem type that
540 represent well the snow climate of the region.

541 **Snow and avalanche climatology**

542 We applied the Mock and Birkeland (2000) algorithm to 40 winter using climatic indicators derived from the
543 CRCM6/SNOWPACK model chain. 33 of the 40 winters were classified as continental and the remaining
544 7 winters as maritime. (Shandro and Haegeli, 2018) apply the (Mock and Birkeland, 2000) algorithm to
545 three area in western Canada: The Coastal mountains (i.e. Whistler), the Columbia's mountains (i.e.
546 Revelstoke) and the Rocky mountains (i.e. Banff). Comparing our snow climate classification results
547 with the three areas in western Canada (Shandro and Haegeli, 2018), each of these three areas never had
548 continental and maritime winters classified in the same area. The Coastal mountains only had maritime

549 and transitional winter. The Columbia's mountains mostly transitional winters with some continental and
550 maritime winters. The Rocky mountains only had continental winters and some transitional winters. Our
551 study area is not similar to western Canada with had continental winters with some maritime winters. From
552 the perspective of seasonal avalanche problem frequency, the Chic-Chocs region exhibits a distribution with
553 around 10% of wet-snow problem types, around 10-20 % and the remaining is mostly wind slab and new
554 snow problem type. This seasonal avalanche problem type frequency was similar to the Coastal Mountains
555 (mostly maritime winters) and the Columbia Mountains (mostly transitional winters). Surprisingly, the
556 Rocky mountains had mostly Continental winters like our study area, but the persistent problem type was
557 more present around 60-70%, compared to 10-20% in the Chic-Chocs.

558 If we compared the climatic indicators of Mock and Birkeland (2000) algorithm with the three classic
559 western region in the United-States, our study area shares similarities with continental regions for all
560 meteorological variables except rain (Figure 4). Other regions of the world, such as Mt. Washington and
561 the central Japanese Alps, exhibit the same pattern of low snowfall, cold air temperatures, and significant
562 precipitation during winter (Figure 4). This suggests that the Chic-Chocs are also influenced by climate
563 factors typical of the continental and maritime snow climates, resulting in snow climate characteristics
564 that do not fit neatly into established classifications of western North America. The sequence from cold
565 temperatures to significant rain is a distinguishing feature that sets these regions apart from classic snow
566 climates of western North America. This dual influence results in snow cover that exhibit characteristics
567 of both continental and maritime climates, such as the presence of faceted crystals and layers of ice due to
568 rain-on-snow events. These mixed characteristics between a continental and maritime winters defined the
569 specific climatic and snow coverconditions of regions such as the Chic-Chocs, Mt. Washington, and the
570 Central Japanese Alps.

571 The snow grain type distribution and climatic conditions of the study area can be compared with those
572 studied in Svalbard, Norway (Eckerstorfer and Christiansen, 2011). Both snow cover are cold and relatively
573 thin ($\approx 1-1.5$ m), dominated by temperature gradient metamorphism processes. These regions experience
574 basal instability and faceted crystals due to cold winter temperatures, and are also affected by maritime
575 depressions that bring warm air and rain, causing ice/melt freeze stratification in the snow cover. Similar
576 to Svalbard, our results showed that the Chic-Chocs region has snow grain types characteristic of both a
577 continental climate (facet and depth hoar) and a maritime climate (ice/melt-freeze layering). Snow and
578 climate data revealed two major snow climate components: a cold snow cover combined with a maritime

579 influence causing rain-on-snow events.

580 Ikeda and others (2009) described two study areas in the Japanese Alps: the Japanese Coastal Moun-
581 tains (Northern Japanese Alps) and the Central Japanese Alps. Their research shows similarities between
582 the Central Japanese Alps and the Chic-Chocs region. Both regions obtained similar snow climate re-
583 sults using the Mock and Birkeland (2000) flow chart: primarily continental winters with some maritime
584 winters (Ikeda and others, 2009). The criteria used for classification are also similar, with a continental
585 winter characterised by a mean December temperature gradient ($\text{meanDEC} > 10^\circ\text{C}$) and a maritime winter
586 characterised by rainfall ($> 80 \text{ mm}$) (Ikeda and others, 2009). The climatic conditions are similar, with
587 cold air temperatures, low snowfall, and significant precipitation (Figure 4). The snow cover structures
588 are comparable, showing a strong prevalence of faceted crystals and melt forms (Ikeda and others, 2009).
589 The authors found that these characteristics did not fit any of the three major snow climate classifications,
590 leading them to propose a new classification for the Central Japanese Alps: the Rainy Continental snow
591 climate. This new classification is defined by the following specific characteristics (Ikeda and others, 2009):

- 592 1) A relatively thin snow cover and cold air temperatures, similar to continental snow climate regions.
- 593 2) Heavy rainfall, comparable to or exceeding that of maritime snow climate regions.
- 594 3) Persistent structural weakness caused by faceted crystals and depth hoar, similar to continental
595 snow climate regions.
- 596 4) The dominance of both faceted crystals and wet grains.

597 Similar to Ikeda and others (2009), our results suggest that the snow climate of the Chic-Chocs does
598 not fit into the three traditional snow climate classifications. Historically, the Chic-Chocs region has been
599 classified as a maritime snow climate according to the Sturm and others (1995) global classification, which
600 is based solely on climatic variables such as temperature and precipitation without considering snow cover
601 or avalanche regimes (Sturm and others, 1995). Other authors have used the term Cold Maritime to
602 describe the region (Fortin and others, 2011; Gauthier and others, 2017).

603 The Chic-Chocs region shares similarities with several regions around the world, such as Mt. Wash-
604 ington and the Central Japanese Alps. All of these regions are influenced by cold air masses from the
605 continent and low-pressure cells from the ocean. These specific influences of both continental and maritime
606 low-pressure cells have previously been observed for the northeastern coast of the United States (Karmosky,
607 2007; Perry and others, 2010). This contrasts with the coastal mountain ranges of the northwestern United

608 States, which are primarily influenced by maritime low-pressure cells. The four characteristics mentioned
609 above for the Rainy Continental classification of the Central Japanese Alps are identical to those observed
610 for the Chic-Chocs. However, the term "Rainy Continental" proposed by Ikeda and others (2009), expresses
611 both continental and maritime influences, similar to a transitional snow climate. However, the term Rainy
612 Continental could be a better fit for insular, peninsular, or northeastern continental regions than any of
613 the three major snow climates developed for the larger mountain ranges of the western United States.

614 Recently, Reuter and others (2023) characterised snow avalanche climate regions in the French Alps
615 by occurrences of avalanche problem types relevant for natural release. They applied the traditional snow
616 climate classification of Mock and Birkeland (2000) and compared the results with a snow avalanche cli-
617 matology based on a clustering analysis of avalanche problem type occurrences. Their analysis revealed
618 4 clusters defined by the number of days with persistent problems, the number of days with new snow
619 problems and the onset date of wet-snow problems. These three factors lead to a combination of 7 possi-
620 bilities, 4 of which they observed in the French Alps, with potentially three more based on their criteria.
621 Based on our clustering analysis, two of our clusters were similar to two of the clusters observed in the
622 French Alps. One cluster was similar to the one in the French Alps and has an average wet-snow activity
623 onset date around February with a relatively low frequency of persistent weak layers (of around 8 days
624 per season) and about 6 days with new snow problems. This cluster was observed in front-range regions
625 on the western flank of the French Alps. A second cluster, similar to the Mont Blanc or the Beaufortain
626 range in the French Alps, had a late wet-snow onset date around the end of April or later, around 13 days
627 with persistent weak layers and 10 days with new snow problems per season. Our study revealed another
628 cluster with a very early wet-snow onset date in December, but with similar frequencies of persistent and
629 new snow problems.

630 Regarding climate change, Eckert and others (2024) reviewed the past and projected effects of climate
631 change on avalanche activity. They found a significant decrease in dry snow avalanches relative to an
632 increase in wet snow avalanches. Currently, more winters are characterised by dry snow situations, such as
633 new snow, wind slabs, and persistent problem types, compared to wet-snow problem types. However, as
634 shown by Eckert and others (2024), these proportions could change towards more situations with wet-snow
635 relative to dry-snow avalanches problems. Giacona and others (2021) observed an upslope shift of avalanche
636 activity, where low altitude mountains saw a reduction in the number and the period of avalanches. This
637 finding suggests that clusters with late onset dates (April) of wet-snow avalanche problems are likely to

638 be affected or disappear in favour of the other two clusters with a mid-season (February) and early wet-
639 snow onset date (December). Today's Chic-Choc snow climate may correspond to the projection of snow
640 climates in other regions, as the Rainy Continental may be the new Continental.

641 **Perspective**

642 Building on the framework developed by Reuter and others (2022, 2023), this study details and charac-
643 terizes the snow and avalanche climate of the Chic-Chocs Range, located in the northeastern Appalachian
644 Mountains of North America. The implementation of the avalanche problem type, derived from 40 winters
645 of SNOWPACK simulations, provided a unique perspective to describe the snow and avalanche climate of
646 the area. As suggested by Shandro and Haegeli (2018) and Reuter and others (2023), using the avalanche
647 problem type introduces a new perspective to propose new classifications for regions that differ from the
648 three conventional snow climates found in western North America. Unlike the geographic clustering study
649 of Reuter and others (2023), our approach was temporal, aiming to identify different "types" of winters that
650 the region may experience. Figure 9-bd illustrates a clustering into three categories over the 40 winters,
651 differing from the continental and maritime 'types' of winters by primarily using the avalanche problem
652 type. This type of research opens the possibility to characterize the snow and avalanche climate where
653 field data are not available. The ERA5 climate model of the European Center for Medium-Range Weather
654 Forecasts (ECMWF), coupled with the SNOWPACK simulation and the method of Reuter and others
655 (2022), represents a new potential framework to analyze new regions that aim to create an historic of
656 potential avalanche problem types to develop a forecasting system based on their climate.

657 **CONCLUSION**

658 This study provides a comprehensive analysis of the snow and avalanche climate in the Chic-Chocs region
659 of the Gaspé Peninsula, as part of the northeastern Appalachians in eastern Canada. Using a variety
660 of methods and data sources, including meteorological observations, snow grain type distributions, and
661 avalanche problem types, we provide a detailed characterization of the region's specific snow and avalanche
662 climate.

663 The snow climate classification results, based on the Mock and Birkeland (2000) flowchart, indicate
664 a predominantly continental climate with occasional maritime winters. This finding contrasts with the
665 more traditional snow climate observed in western North America, highlighting the specificity of the Chic-

666 Chocs region. Our comparison with similar regions around the world, such as Mt. Washington and
667 the central Japanese Alps, revealed patterns of low snowfall, cold air temperatures, and significant rain
668 precipitation. This similarity suggests that the Chic-Chocs, like these other regions, do not fit neatly into
669 traditional classifications of continental, maritime, or transitional snow climates. Furthermore, comparison
670 with Svalbard, Norway, underscored the presence of cold, thin snow cover dominated by faceted crystals and
671 basal instability, influenced by both cold winter temperatures and maritime depressions. These conditions
672 result in a snow cover structure characterised by both continental and maritime elements, such as faceted
673 crystals and ice/melt freeze layers.

674 The inclusion of avalanche problem types derived from 40 winters of snow cover simulations (CRCM6-
675 SNOWPACK) provided seasonal patterns of natural snow instability mostly dependant on the month
676 where the wet-snow problem type occurs. We were able to compare our results with another study in the
677 French Alps and discuss a classification/cluster exclusively around avalanche problem type, shifting from
678 the traditional climate-based description. This study highlights the potential of snow cover modeling and
679 avalanche problem type methodology to improve our understanding and classification of snow climates,
680 ultimately contributing to improved avalanche forecasting and risk management in regions with similar
681 complex dynamics. Finally, in our broader perspective of climate change, where rain and wet-snow problem
682 type may become more common for continental regions around the world, the Rainy Continental of the
683 Chic-chocs may be the new Continental around the world.

684 **ACKNOWLEDGEMENTS**

685 We would like to thank Dominic Boucher, Julie Leblanc and Jean-Pierre Gagnon from Avalanche Québec
686 for providing us their meteorological and forecast dataset. We also want to acknowledge them for all the
687 discussion based on their 20 years of expertise of the Chic-Chocs area.

688 **REFERENCES**

- 689 Armstrong RL and Armstrong BR (1987) Snow and avalanche climates of the western United States: a comparison
690 of maritime, intermountain and continental conditions. *IAHS publication*, **162**, 281–294
- 691 AWSOME Core Team (2024) AWSOME: Avalanche Warning Service Operational Meteo Environment (doi:
692 <https://gitlab.com/avalanche-warning>)
- 693 Baggi S and Schweizer J (2009) Characteristics of wet-snow avalanche activity: 20 years of observations from a high

- 694 alpine valley (Dischma, Switzerland). *Natural Hazards*, **50**(1), 97–108, ISSN 0921-030X (doi: 10.1007/s11069-008-
695 9322-7)
- 696 Bellaire S and Jamieson B (2013) Forecasting the formation of critical snow layers using a coupled
697 snow cover and weather model. *Cold Regions Science and Technology*, **94**, 37–44, ISSN 0165232X (doi:
698 10.1016/j.coldregions.2013.06.007)
- 699 Bellaire S, Jamieson JB and Fierz C (2011) Forcing the snow-cover model SNOWPACK with forecasted weather
700 data. *Cryosphere*, **5**(4), 1115–1125, ISSN 19940416 (doi: 10.5194/tc-5-1115-2011)
- 701 Conway H and Wilbour C (1999) Evolution of snow slope stability during storms. *Cold Regions Science and Tech-*
702 *nology*, **30**(1-3), 67–77, ISSN 0165232X (doi: 10.1016/S0165-232X(99)00009-9)
- 703 Côté K, Madore JB and Langlois A (2017) Uncertainties in the SNOWPACK multilayer snow model for a Canadian
704 avalanche context: sensitivity to climatic forcing data. *Physical Geography*, **38**(2), 124–142, ISSN 02723646 (doi:
705 10.1080/02723646.2016.1277935)
- 706 EAWS (2019) Avalanche Problems, EAWS - European Avalanche Warning Services.
- 707 Eckerstorfer M and Christiansen H (2011) The "high arctic maritime snow climate" in Central svalbard. *Arctic,*
708 *Antarctic, and Alpine Research*, **43**(1), 11–21, ISSN 15230430 (doi: 10.1657/1938-4246-43.1.11)
- 709 Eckert N, Corona C, Giacona F, Gaume J, Mayer S, van Herwijnen A, Hagenmuller P and Stoffel M (2024) Climate
710 change impacts on snow avalanche activity and related risks. *Nature Reviews Earth & Environment*, **5**(5), 369–389,
711 ISSN 2662-138X (doi: 10.1038/s43017-024-00540-2)
- 712 Fortin G and Héту B (2014) Estimating winter trends in climatic variables in the Chic-Chocs Mountains, Canada
713 (1970-2009). *International Journal of Climatology*, **34**(10), 3078–3088, ISSN 10970088 (doi: 10.1002/joc.3895)
- 714 Fortin G, Héту B and Germain D (2011) Climat Hivernal et Régimes avalanches dans le corridors routier de la
715 gaspésie septentrionale (Québec, Canada). *Climatologie*, **8** (doi: 10.4267/climatologie.202)
- 716 Gagnon RM (1970) Le climat des Chic-Chocs. Technical report, Ministère des Richesses naturelles du Québec, Service
717 de la météorologie
- 718 Gaume J, Van Herwijnen A, Chambon G, Wever N and Schweizer J (2017) Snow fracture in relation to slab
719 avalanche release: Critical state for the onset of crack propagation. *Cryosphere*, **11**(1), 217–228, ISSN 19940424
720 (doi: 10.5194/tc-11-217-2017)
- 721 Gauthier F, Germain D and Héту B (2017) Logistic models as a forecasting tool for snow avalanches in a cold
722 maritime climate: northern Gaspésie, Québec, Canada. *Natural Hazards*, **89**(1), 201–232, ISSN 0921-030X (doi:
723 10.1007/s11069-017-2959-3)

- 724 Germain D, Filion L and Hétu B (2009) Snow avalanche regime and climatic conditions in the Chic-Choc Range,
725 eastern Canada. *Climatic Change*, **92**(1-2), 141–167, ISSN 0165-0009 (doi: 10.1007/s10584-008-9439-4)
- 726 Germain D, Hétu B and Fillion L (2010) Tree-ring based reconstruction of past snow avalanche events and risk
727 assessment in Northern Gaspé Peninsula (Québec, Canada). In *Tree Rings and Natural Hazards: A State-of-Art*,
728 51–73, Springer
- 729 Giacona F, Eckert N, Corona C, Mainieri R, Morin S, Stoffel M, Martin B and Naaim M (2021) Upslope migration
730 of snow avalanches in a warming climate. *Proceedings of the National Academy of Sciences of the United States of*
731 *America*, **118**(44), ISSN 10916490 (doi: 10.1073/PNAS.2107306118/FORMAT/EPUB)
- 732 Girard C, Plante A, Desgagné M, McTaggart-Cowan R, Côté J, Charron M, Gravel S, Lee V, Patoine A, Qaddouri
733 A, Roch M, Spacek L, Tanguay M, Vaillancourt PA and Zadra A (2014) Staggered Vertical Discretization of the
734 Canadian Environmental Multiscale (GEM) Model Using a Coordinate of the Log-Hydrostatic-Pressure Type.
735 *Monthly Weather Review*, **142**(3), 1183–1196, ISSN 0027-0644 (doi: 10.1175/MWR-D-13-00255.1)
- 736 Gray J, Davesne G, Fortier D and Godin E (2017) The Thermal Regime of Mountain Permafrost at the Summit
737 of Mont Jacques-Cartier in the Gaspé Peninsula, Québec, Canada: A 37 Year Record of Fluctuations show-
738 ing an Overall Warming Trend. *Permafrost and Periglacial Processes*, **28**(1), 266–274, ISSN 10456740 (doi:
739 10.1002/ppp.1903)
- 740 Haegeli P and McClung DM (2007) Expanding the snow-climate classification with avalanche-relevant information:
741 Initial description of avalanche winter regimes for southwestern Canada. *Journal of Glaciology*, **53**(181), 266–276,
742 ISSN 00221430 (doi: 10.3189/172756507782202801)
- 743 Hägeli P and McClung DM (2003) Avalanche characteristics of a transitional snow climate-Columbia Moun-
744 tains, British Columbia, Canada. *Cold Regions Science and Technology*, **37**(3), 255–276, ISSN 0165232X (doi:
745 10.1016/S0165-232X(03)00069-7)
- 746 Heierli J, Gumbsch P and Zaiser M (2008) Anticrack nucleation as triggering mechanism for snow slab avalanches.
747 *Science*, **321**(5886), 240–243, ISSN 00368075 (doi: 10.1126/science.1153948)
- 748 Hétu B (2010) Les conditions météorologiques propices au déclenchement des avalanches de neige dans les corridors
749 routiers du nord de la Gaspésie, Québec, Canada. *Géographie physique et Quaternaire*, **61**(2-3), 165–180, ISSN
750 1492-143X (doi: 10.7202/038990ar)
- 751 Ikeda S, Wakabayashi R, Izumi K and Kawashima K (2009) Study of snow climate in the Japanese Alps:
752 Comparison to snow climate in North America. *Cold Regions Science and Technology*, **59**, 119–125 (doi:
753 10.1016/j.coldregions.2009.09.004)

- 754 Imbach B, Gauthier F and Langlois A (2024) What are the impacts of climate change on the properties and stability
755 of the snowpack? In *Colloque annuel du Centre d'Étude Nordique CEN*, Québec
- 756 Karmosky C (2007) Synoptic climatology of snowfall in the northeastern United States: an analysis of snowfall
757 amounts from diverse synoptic weather types
- 758 LaChapelle ER (1965) Avalanche forecasting-a modern synthesis. Technical report, US Department of Agriculture
- 759 Lehning M, Bartelt P, Brown B, Russi T, Stockli U and Zimmerli M (1999) SNOWPACK model calculations for
760 avalanche warning based upon a new network of weather and snow stations. *Cold Regions Science and Technology*,
761 **30**, 145–157
- 762 Macqueen J (1967) Some methods for classification and analysis of multivariate observations. In *Proceedings of the*
763 *Fifth Berkeley Symposium on Mathematical Statistics and Probability, Volume 1: Statistics*
- 764 Madore JB, Langlois A and Côté K (2018) Evaluation of the SNOWPACK model's metamorphism and
765 microstructure in Canada: a case study. *Physical Geography*, **39**(5), 406–427, ISSN 02723646 (doi:
766 10.1080/02723646.2018.1472984)
- 767 Madore JB, Fierz C and Langlois A (2022) Investigation into percolation and liquid water content in a multi-layered
768 snow model for wet snow instabilities in Glacier National Park, Canada. *Frontiers in Earth Science*, **10**, ISSN
769 2296-6463 (doi: 10.3389/feart.2022.898980)
- 770 McClung D and Schaerer P (2006) *The avalanche Handbook*. The Mountaineers Books
- 771 McTaggart-Cowan R, Vaillancourt PA, Zadra A, Chamberland S, Charron M, Corvec S, Milbrandt JA, Paquin-Ricard
772 D, Patoine A, Roch M, Separovic L and Yang J (2019) Modernization of Atmospheric Physics Parameterization
773 in Canadian NWP. *Journal of Advances in Modeling Earth Systems*, **11**(11), 3593–3635, ISSN 19422466 (doi:
774 10.1029/2019MS001781)
- 775 Meloche F (2019) Variabilité spatio-temporelle des propriétés du manteau neigeux dans un contexte opérationnel de
776 prévision des avalanches, Gaspésie, Canada
- 777 Mitterer C and Schweizer J (2013) Analysis of the snow-atmosphere energy balance during wet-snow instabilities and
778 implications for avalanche prediction. *The Cryosphere*, **7**(1), 205–216, ISSN 1994-0424 (doi: 10.5194/tc-7-205-2013)
- 779 Mitterer C, Heilig A, Schmid L, Van Herwijnen A, Eisen O and Schweizer J (2016) Comparison of measured and
780 modeled snow cover liquid water content to improve local wet-snow avalanche prediction. In *International Snow*
781 *Science Workshop, Breckenridge, Colorado*

- 782 Mock CJ and Birkeland KW (2000) Snow Avalanche Climatology of the Western United States Mountain
783 Ranges. *Bulletin of the American Meteorological Society*, **81**(10), 2367–2392 (doi: [https://doi.org/10.1175/1520-0477\(2000\)081<2367:SACOTW>2.3.CO;2](https://doi.org/10.1175/1520-0477(2000)081<2367:SACOTW>2.3.CO;2))
- 785 Moreno-Ibáñez M, Laprise R and Gachon P (2023) Assessment of simulations of a polar low with the Canadian
786 Regional Climate Model. *PLOS ONE*, **18**(10), e0292250, ISSN 1932-6203 (doi: [10.1371/journal.pone.0292250](https://doi.org/10.1371/journal.pone.0292250))
- 787 Perry LB, Konrad CE, Hotz DG and Lee LG (2010) Synoptic Classification of Snowfall Events in the Great Smoky
788 Mountains, USA. *Physical Geography*, **31**(2), 156–171, ISSN 0272-3646 (doi: [10.2747/0272-3646.31.2.156](https://doi.org/10.2747/0272-3646.31.2.156))
- 789 Reuter B, Viallon-Galinier L, Horton S, Van Herwijnen A, Mayer S, Hagenmuller P and Morin S (2022) Characterizing
790 snow instability with avalanche problem types derived from snow cover simulations. *Cold Regions Science and
791 Technology*, **194**, 103462 (doi: [10.1016/j.coldregions.2021.103462](https://doi.org/10.1016/j.coldregions.2021.103462))
- 792 Reuter B, Hagenmuller P and Eckert N (2023) Snow and avalanche climates in the French Alps using avalanche
793 problem frequencies. *Journal of Glaciology*, **69**, ISSN 1292-1304 (doi: [10.1017/jog.2023.23](https://doi.org/10.1017/jog.2023.23))
- 794 Richter B, Schweizer J, Rotach M and van Herwijnen A (2019) Validating modeled critical crack length for crack
795 propagation in the snow cover model SNOWPACK. *The Cryosphere*, **13**(June), 3353–3366 (doi: [10.5194/tc-2019-97](https://doi.org/10.5194/tc-2019-97))
- 797 Roberge F, Luca AD, Laprise R, Lucas-Picher P and Thériault J (2024) Spatial spin-up of precipitation in limited-
798 area convection-permitting simulations over North America using the CRCM6/GEM5.0 model. *Geosci. Model Dev*,
799 **17**, 1497–1510 (doi: [10.5194/gmd-17-1497-2024](https://doi.org/10.5194/gmd-17-1497-2024))
- 800 Roch A (1949) Report on snow and avalanche conditions in U.S.A Western ski resorts. Technical report, Swissfeder-
801 alInstituteforSnowandAvalanche, Davos
- 802 Schweizer J, Jamieson JB and Schneebeli M (2003) Snow avalanche formation. *Reviews of Geophysics*, **41**(4), 3–5,
803 ISSN 87551209 (doi: [10.1029/2002RG000123](https://doi.org/10.1029/2002RG000123))
- 804 Shandro B and Haegeli P (2018) Characterizing the nature and variability of avalanche hazard in western Canada.
805 *Natural Hazards and Earth System Sciences*, **18**(4), 1141–1158, ISSN 16849981 (doi: [10.5194/nhess-18-1141-2018](https://doi.org/10.5194/nhess-18-1141-2018))
- 806 Statham G, Haegeli P, Greene E, Birkeland K, Israelson C, Tremper B, Stethem C, McMahon B, White B and
807 Kelly J (2018) A conceptual model of avalanche hazard. *Natural Hazards*, **90**(2), 663–691, ISSN 15730840 (doi:
808 [10.1007/s11069-017-3070-5](https://doi.org/10.1007/s11069-017-3070-5))
- 809 Sturm M, Holmgren J and Liston GE (1995) A Seasonal Snow Cover Classification System for Lo-
810 cal to Global Applications. *Journal of Climate*, **8**(5), 1261–1283, ISSN 0894-8755 (doi: [10.1175/1520-0442\(1995\)008<1261:ASSCCS>2.0.CO;2](https://doi.org/10.1175/1520-0442(1995)008<1261:ASSCCS>2.0.CO;2))

- 812 Techel F, Karsten M and Schweizer J (2020) On the importance of snowpack stability, the frequency distribution
813 of snowpack stability, and avalanche size in assessing the avalanche danger level. *Cryosphere*, **14**(10), 3503–3521,
814 ISSN 19940424 (doi: 10.5194/TC-14-3503-2020)
- 815 Vionnet V, Brun E, Morin S, Boone A, Faroux S, Le Moigne P, Martin E and Willemet JM (2012) The detailed
816 snowpack scheme Crocus and its implementation in SURFEX v7.2. *Geoscientific Model Development*, **5**(3), 773–
817 791, ISSN 1991-9603 (doi: 10.5194/gmd-5-773-2012)